UNITED STATES DEPARTMENT OF COMMERCE
JESSE H. JONES, Secretary
NATIONAL BUREAU OF STANDARDS
Lyman J. Briggs, Director

✦

# Journal of Research

## of the

## National Bureau of Standards

✦

Volume 29, Number 3
September 1942

[Published with approval of the Director of the Budget]

UNITED STATES
GOVERNMENT PRINTING OFFICE
WASHINGTON : 1942

For sale by the Superintendent of Documents, Washington, D. C. - - - - - - Price 30 cents
$3.50 per year on subscription

The prices of the separate Research Papers appearing in this JOURNAL are given on the front cover page. If 100 or more copies of any separate are ordered, a discount of 25 percent is allowed. Those who desire copies of separate Research Papers should send their orders and remittances without delay to the Superintendent of Documents, U. S. Government Printing Office, Washington, D. C. This will aid him to determine the number of copies to be printed for sale. Research Papers are not printed from electrotypes, and usually no more reprints can be had when the first and only printing is exhausted.

## MATHEMATICAL TABLES

A list of the mathematical tables now obtainable from the National Bureau of Standards is printed on pages 3 and 4 of the Journal cover. New tables will be announced from time to time as they become available.

U. S. DEPARTMENT OF COMMERCE NATIONAL BUREAU OF STANDARDS

RESEARCH PAPER RP1495

*Part of Journal of Research of the National Bureau of Standards, Volume 29, September 1942*

# PROVISIONAL pH VALUES FOR CERTAIN STANDARD BUFFER SOLUTIONS

By Roger G. Bates, Walter J. Hamer, George G. Manov, and S. F. Acree

ABSTRACT

For use in the calibration of electrometric pH assemblies, 17 standard buffer solutions have been investigated, and pH values at 20°, 25°, and 30° C have been assigned to them. The pH values of these solutions range from 2.27 to 11.68 and are considered accurate to ±0.02 pH unit.

Hydrogen–silver-chloride cells without liquid junctions were used for establishing the precise pH values of the buffer mixtures. The assumptions made to determine the activity coefficients of the ions in the mixtures are discussed. The method of assigning an accurate pH value to a buffer mixture is outlined.

Directions for preparing the mixtures from purified anhydrous salts, standard solutions of acid and alkali, and pure water are given. Changes of temperature have a larger effect on the pH values of the buffers of pH greater than 7 than on those of the acid buffers. In all cases the effect of dilution is small; an error of 1 percent in the volume of solvent added results in a change of less than 0.001 pH unit.

The use of a pH meter of the glass-electrode–calomel-electrode type calibrated by means of a standard buffer may often involve greater uncertainties than those inherent in the pH value assigned to the buffer mixture. It should be recognized that errors arising from liquid junction, hysteresis, temperature, and salt effects may combine to give an uncertainty of 0.01 and 0.03 unit or more in practical pH tests.

CONTENTS

| | Page |
|---|---|
| I. Recommended buffer solutions | 183 |
| II. Preparation of reagents and solutions | 185 |
| III. Sources of error in the use of pH meters calibrated with standard buffers | 186 |
| IV. Accuracy of the standard pH values | 188 |
| V. References | 190 |

## I. RECOMMENDED BUFFER SOLUTIONS

In the practice of determining pH (the negative common logarithm of the hydrogen-ion activity) by electrometric methods, the electrode system is usually standardized by means of buffer solutions of known acidity. Standard reference solutions used in the calibration of such pH equipment must be easily reproducible in composition, and stable, so that the pH values accurately established for them by means of the hydrogen electrode can be used with confidence.

The pH Standards Section of the National Bureau of Standards has in progress the selection and standardization of suitable substances of requisite purity and stability. The thermodynamic ionization constants of the weak acids which form useful buffer mixtures are being determined at temperatures between 0° and 60° C from electromotive-force measurements of hydrogen–silver-chloride cells without liquid junction. These measurements likewise yield information regarding the activity coefficients of the ions which compose the mixture. The evaluation of the pH numbers from the electromotive-force measurements for each buffer solution is then possible. The

description of the method and its application to the determination of the pH values of malonate-chloride mixtures have been given in detail by Hamer and Acree [1] * and by Hamer, Burton, and Acree [2]. It is expected that pure crystalline buffer salts to cover the useful pH range in intervals of 0.2 pH unit will ultimately be available.

In table 1 are listed pH values of 17 mixtures at 20°, 25°, and 30° C. All of the values are thought to be accurate within ±0.02 unit. Compositions are given in table 1 in molalities (moles per kilogram of water); those of table 2 are given in terms of moles of alkali or acid and weight of water and of anhydrous buffer salt required for the accurate preparation of the solutions. For work which requires more than one ionic strength, different concentrations of certain buffers having nearly the same pH values are given. In the articles giving the precise data on which the tabulated values are based, the pH values at 0° to 60° C in 5° steps will be given to within 0.001 to 0.002 unit for concentrations of buffers from 0.1 to 0.001 *M*.

TABLE 1.—pH *values of standard buffer mixtures at 20°, 25°, and 30° C*

| Solution No. | Standard buffer mixture | Molalities | | | pH value | | |
|---|---|---|---|---|---|---|---|
| | | $m_1$ | $m_2$ | $m_3$ | 20° | 25° | 30° |
| 1 | $KH_2PO_4$ ($m_1$), HCl ($m_2$) | 0.01549 | 0.01221 | | 2.262 | 2.270 | 2.280 |
| 2 | | .01105 | .008710 | | 2.358 | 2.366 | 2.373 |
| 3 | $HKC_8H_4O_4$ (acid potassium phthalate) ($m_1$), HCl ($m_2$) | .03600 | .01800 | | 3.002 | 3.009 | 3.017 |
| 4 | $HKC_8H_4O_4$ (acid potassium phthalate) ($m_1$) | .05000 | | | 4.001 | 4.008 | 4.015 |
| 5 | $HKC_8H_4O_4$ (acid potassium phthalate) ($m_1$) KOH ($m_2$), KCl ($m_3$) | .1000 | .0600 | 0.04000 | 4.633 | 4.629 | 4.628 |
| 6 | | .03000 | .02000 | .01000 | 5.071 | 5.069 | 5.071 |
| 7 | $CH_2(COOH)_2$ (malonic acid) ($m_1$), NaOH ($m_2$) NaCl ($m_3$) | .02000 | .03000 | .01000 | 5.434 | 5.444 | 5.454 |
| 8 | | .01400 | .02100 | .007000 | 5.466 | 5.476 | 5.487 |
| 9 | $KH_2PO_4$ ($m_1$), $Na_2HPO_4$ ($m_2$), NaCl ($m_3$) | .02877 | .01834 | .02877 | 6.658 | 6.640 | 6.630 |
| 10 | | .02000 | .03000 | .02000 | 7.012 | 6.994 | 6.983 |
| 11 | $NaH_2PO_4$ ($m_1$), $Na_2HPO_4$ ($m_2$), NaCl ($m_3$) | .002943 | .004501 | .002943 | 7.218 | 7.202 | 7.190 |
| 12 | *p*-$HOC_6H_4SO_3K$ (potassium *p*-phenolsulfonate) ($m_1$), NaOH ($m_2$), NaCl ($m_3$) | .01896 | .009539 | .009419 | 8.902 | 8.848 | 8.798 |
| 13 | | .01168 | .005875 | .005801 | 8.933 | 8.879 | 8.828 |
| 14 | $Na_2B_4O_7$ ($m_1$), NaCl ($m_2$) | .006045 | .01210 | | 9.210 | 9.165 | 9.124 |
| 15 | | .004731 | .009465 | | 9.212 | 9.168 | 9.127 |
| 16 | $Na_2HPO_4$ ($m_1$), NaOH ($m_2$), NaCl ($m_3$) | .01213 | .009303 | .003022 | 11.76 | 11.62 | ..... |
| 17 | | .01796 | .01377 | .004474 | 11.82 | 11.68 | ..... |

TABLE 2.—*Compositions of the standard buffer mixtures*

| Solution No. | Composition [1] (Amounts to be added to 1 kg of $H_2O$) |
|---|---|
| 1 | 2.108 g $KH_2PO_4$; 0.01221 mole HCl. |
| 2 | 1.504 g $KH_2PO_4$; 0.008710 mole HCl. |
| 3 | 7.352 g $HKC_8H_4O_4$ (acid potassium phthalate); 0.018 mole HCl. |
| 4 | 10.211 g $HKC_8H_4O_4$ (acid potassium phthalate). |
| 5 | 20.422 g $HKC_8H_4O_4$ (acid potassium phthalate); 0.06 mole KOH; 2.982 g KCl. |
| 6 | 6.126 g $HKC_8H_4O_4$ (acid potassium phthalate); 0.02 mole KOH; 0.746 g KCl. |
| 7 | 2.081 g $CH_2(COOH)_2$ (malonic acid); 0.03 mole NaOH; 0.585 g NaCl. |
| 8 | 1.457 g $CH_2(COOH)_2$ (malonic acid); 0.021 mole NaOH; 0.409 g NaCl. |
| 9 | 3.915 g $KH_2PO_4$; 2.604 g $Na_2HPO_4$; 1.682 g NaCl. |
| 10 | 2.722 g $KH_2PO_4$; 4.260 g $Na_2HPO_4$; 1.169 g NaCl. |
| 11 | 0.3630 g $NaH_2PO_4$; 0.6390 g $Na_2HPO_4$; 0.172 g NaCl. |
| 12 | 4.025 g *p*-$HOC_6H_4SO_3K$ (potassium *p*-phenolsulfonate); 0.009539 mole NaOH; 0.551 g NaCl. |
| 13 | 2.479 g *p*-$HOC_6H_4SO_3K$ (potassium *p*-phenolsulfonate); 0.005875 mole NaOH; 0.339 g NaCl. |
| 14 | 1.217 g $Na_2B_4O_7$; 0.707 g NaCl. |
| 15 | 0.9520 g $Na_2B_4O_7$; 0.553 g NaCl. |
| 16 | 1.456 g $Na_2HPO_4$; 0.009303 mole NaOH; 0.177 g NaCl. |
| 17 | 2.155 g $Na_2HPO_4$; 0.01377 mole NaOH; 0.262 g NaCl. |

[1] For practical work, these amounts can be used in a liter of solution.

* Figures in brackets indicate the literature references at the end of this paper.

## II. PREPARATION OF REAGENTS AND SOLUTIONS

All of the salts required for the preparation of these buffer solutions can be purified by recrystallization from water. Purified potassium dihydrogen phosphate, potassium *p*-phenolsulfonate, *p*-$HOC_6H_4SO_3K$, sodium chloride, and potassium chloride can be powdered and dried to the anhydrous state at 110° C. Sodium dihydrogen phosphate and disodium hydrogen phosphate should be dried at room temperature, or slightly above, for a day or more before complete dehydration at 110° is attempted. In this way fusion of the hydrated salts can be avoided. Borax can be dehydrated by fusion in platinum. Acid potassium phthalate, *o*-$HKC_8H_4O_4$, is supplied by the National Bureau of Standards as Standard Sample 84a. It is suggested that malonic acid, $CH_2(COOH)_2$, be purified by washing it with carbon tetrachloride and by recrystallizing it from ether. To avoid decomposition, the acid and its solutions should not be heated above 66° C.

A carbonate-free stock solution of sodium hydroxide can be prepared by the dilution of a 50-percent solution of sodium hydroxide of reagent quality (filtered to remove the insoluble carbonate) with freshly boiled distilled water. Carbonate can be removed from a 50-percent solution of potassium hydroxide by the dropwise addition of a strong solution of barium hydroxide until no more precipitate is formed. The barium carbonate precipitate should be allowed to settle overnight in a stoppered bottle and the clear solution siphoned off and diluted with carbon-dioxide-free water. The alkali solutions should be standardized against benzoic acid or acid potassium phthalate (NBS Standard Samples 39e and 84a). A solution of hydrochloric acid may then be standardized by titration against one of the standard alkalies. Phenolphthalein will serve as an indicator in each of these titrations. Precautions should be taken to prevent carbon dioxide from the air from gaining access to the titration vessel or to the bottle in which the standard alkali is stored.

The buffer solutions should be prepared with freshly boiled distilled water. It may be boiled in a large flask which can be closed during cooling by means of a stopper which bears a soda-lime tube. In this way the danger of contamination of the water with carbon dioxide is avoided.

Buffers having pH values near the neutral point or on the acid side should be stored in glass-stoppered bottles of resistant glass. It is suggested that alkaline buffers be kept in alkali-resistant bottles or flasks equipped with a siphon, and with a soda-lime guard tube at the air intake, which permits withdrawal of the solution without the introduction of carbon dioxide.

Six-tenths gram of thymol dissolved in each liter of buffer solution prevents mold growth, but the pH values of the alkaline buffers will be altered slightly. The magnitude of the pH change attendant on the addition of thymol to the standard buffer may be determined by comparing, by means of a pH meter, the pH value of the untreated buffer solution with that of a portion of the mixture to which has been added the proper quantity of preservative. The meter need not be accurately standardized for the measurement of this small change of pH.

## III. SOURCES OF ERROR IN THE USE OF pH METERS CALIBRATED WITH STANDARD BUFFERS

Measurements of pH with the glass electrode are ordinarily made at temperatures between 20° and 40° C. The instrument must be calibrated at the temperature of use. These standard buffers are intended only for comparison with dilute aqueous solutions, and the pH value of an alcohol-water mixture or of a nonaqueous solution cannot be determined reliably with an apparatus calibrated by their means.

It is apparent from an inspection of table 1 that the temperature must be controlled if the highest reproducibility in the pH of the standard solution is to be attained. Most of the acid buffer solutions increase in pH, and the alkaline buffers decrease in pH, with rise in temperature from 20° to 30° C. It may be noted that at room temperature those buffers having pH values on the acid side of the neutral point show a smaller change with temperature than do those of high pH. For a precision of 0.02 pH unit, the measurement of pH values above 7.3 must be made at temperatures controlled within 2 degrees, and to within 1 degree when the most alkaline phosphate solutions are being employed. For measurements on the acid side, control to 5 degrees is sufficient for the attainment of the same degree of precision. A correction must be made for the electromotive force of the reference electrode at its temperature [5], including the liquid-junction potential (see p. 188). The change in pH with rise in temperature of each buffer can be computed from table 1.

The pH value of a buffer mixture composed of a weak acid and its salt is a function of (a) the ionization constant of the weak acid, (b) the ratio of acid to salt, and (c) a "salt-effect" term which depends upon the total amount and type of ionized substance present. The change of the pH value with temperature is largely the result of the change in the ionization constant. The salt-effect term is small for dilute solutions. On the other hand, accidental errors which alter the ratio of acid to salt are serious. Of these, contamination of the alkaline mixtures with carbon dioxide is the most common source of error. A carbon dioxide-free atmosphere should be employed when possible, but use of the buffer in air within 10 minutes after its removal from the bottle will ordinarily be permissible.

The addition of water in too large or too small a quantity has a relatively small effect, as an inspection of the data of table 1 will indicate. A dilution of 1 percent corresponds to a change of the order of 0.001 pH unit. For this reason, the standard buffers may be prepared with an error less than 0.002 pH unit by dilution to a total volume of 1 liter instead of by the addition of a kilogram of water.

The electromotive-force values of the buffers were determined with a precision corresponding to 0.001 to 0.002 pH in cells without liquid junctions, and the pH values assigned to them probably have an accuracy well within $\pm 0.02$ unit. In the practical use of these buffers, however, in the calibration of vacuum-tube pH meters that have calomel and glass electrodes, the following additional sources of error may be present:

(1) The liquid-junction potentials between the unknown solutions and the reference electrode, such as the saturated KCl-$Hg_2Cl_2$-Hg system, may differ considerably from those between the standard

buffer solution and the same reference electrode. This error may range from 0.01 to 0.03 pH. When strong acid or alkaline solutions are being measured, however, this error may amount to 0.1 to 0.3 pH unit.

(2) The uncertainties in the temperature equilibrium and the hysteresis in the calomel and glass-electrode systems. Even with normal precautions these errors may range from 0.01 to 0.03 pH.

(3) Slow attainment of equilibrium in the double layer at the surface of the glass electrode under certain conditions. This disturbing hysteresis is manifested in a calibration "drift" after the glass electrode is removed from a buffer solution of known pH, rinsed once with distilled water or a second buffer, and then placed in the second buffer, which may or may not have the same hydrogen-ion activity. The electrode should be tested in consecutive small portions of the standard buffer or unknown solution until the drift disappears. This electromotive-force drift may be caused by adsorption of ions from the preceding solution, and to some extent by reactions of the 015 glass with the $Na^+$, $OH^-$ or other ions in solution, and is especially disturbing when the electrode is calibrated in 0.01 to 0.05 *M* buffer and then used in very dilute unknown solutions.

An apparent reproducibility of 0.01 in pH readings may indicate that the factors (1), (2), and (3) are temporarily constant. The error of the measurement, however, may be much larger than 0.01 pH unit, even though the instrument has been calibrated with precise buffer standards.

For the calibration of glass-electrode assemblies, it is important to choose buffers which have pH values and compositions close to those of the unknown mixtures. This precaution is of particular importance at pH values above 9.5, where the "alkali error" of the 015 glass electrode is large. It is hoped that the pH values assigned to the borate and phosphate standards will be especially valuable in calibrations of glass electrodes for tests of alkaline solutions such as boiler waters. For a precision of 0.05 pH, the 015 glass electrode, when calibrated with standard borax buffer, may be used up to pH 9.5 and 10.5 in solutions containing 1 *N* and 0.1 *N* sodium ions, respectively. For the same precision, the standard buffer and an unknown mixture containing 0.1 *N* sodium ion should have pH values differing by 0.1 or less above pH 11.7 to minimize the effects of hysteresis of the glass electrode.

The pH value as read from a pH meter of the glass-electrode–calomel type with liquid junction is expressed approximately by

$$\mathrm{pH} = \frac{(E - E^\circ - Ej)F}{2.3026RT},$$

where $E$ is the electromotive force between the electrodes of the assembly consisting of inner reference electrode, glass, unknown solution, liquid junction, saturated KCl, $Hg_2Cl_2$, and Hg; $E^\circ$ is the standard potential of the cell; $E_j$ is the potential of the liquid junction between saturated KCl and the solution of unknown pH; and $R$, $T$, and $F$ are recognized constants.

It is assumed that the asymmetry potential of the glass electrode has been compensated by calibration of the instrument with a known

buffer and that it remains constant. At 25° C the above equation becomes

$$\text{pH}=(E-E^\circ-E_j)/0.05914.$$

According to almost universal practice, the instrument is calibrated with a standard solution of known pH value, and $E^\circ$ and $E_j$ are assumed to remain constant for the subsequent measurement of unknown solutions. The instrument is adjusted to the "theoretical slope," that is, 0.05914 at 25° C. Thus it is assumed that any solution whose electromotive-force value differs from that of the standard solution by 0.05914 volt at 25° C will have a pH value 1 unit larger or smaller than that of the standard. Adjustments may be made for other theoretical slopes corresponding to the value of 2.3026 $RT/F$ at any temperatures at which the instrument may be used. In most commercial instruments this adjustment is made either automatically or by a temperature-control knob.

Fairly concordant values of $E^\circ-E_j$ have been obtained from measurements of several weak acid buffers having pH values ranging from 2.6 to 9.2 [3, 4]. Measurements of strong acid-salt mixtures, however, suggest that $E_j$ for these solutions may differ by 1 to 3 millivolts (0.01 to 0.05 pH unit) from the value established by calibration with a standard buffer [3, 5]. In such cases, the simple theoretical relation between pH and electromotive force at that temperature is in error, and the measured pH value will differ from the true value. This error may be minimized by calibrating the instrument with the use of a standard buffer having pH value and ion mobilities and concentrations as close as possible to those of the unknown. The fact that the theoretical slope is practically that found experimentally gives assurance for the future of accurate pH measurements, when standards are available for calibration at pH values near those of the unknown solutions.

Until these sources of error are evaluated by extensive precision work, it is better to recognize uncertainties of 0.01 to 0.03 pH unit or more in practical pH tests. This uncertainty is always present in measurements of solutions whose ion concentrations, dielectric constants, liquid-junction potentials, etc., are not known.

## IV. ACCURACY OF THE STANDARD pH VALUES

To obtain the pH of a standard buffer mixture containing known quantities of chlorides, as illustrated in table 2, use is made of the fact that the electromotive force ($E$) between the hydrogen and silver-silver-chloride electrodes is related to the pH value [1, 2] by four equations which involve the ionization constant of the buffer acid, HAn; the concentration of the acid and of its salts; and the activity coefficients of the various ions involved in the reactions:

$$\text{pH}=\frac{(E-E^\circ)F}{2.3026\,RT}+\log m_{\text{Cl}}+\log f_{\text{Cl}}, \tag{1}$$

$$\frac{(E-E^\circ)F}{2.3026\,RT}+\log m_{\text{Cl}}+\log (m_{\text{HAn}}/m_{\text{An}})=\text{p}K-\log(f_{\text{Cl}}f_{\text{HAn}}/f_{\text{An}}), \tag{2}$$

$$\log f_i=\frac{-Az_i^2\sqrt{\mu}}{1+Ba_i\sqrt{\mu}}+\beta\mu, \tag{3}$$

$$\text{pH}=\text{p}K-\log (m_{\text{HAn}}/m_{\text{An}})+\log (f_{\text{An}}/f_{\text{HAn}}). \tag{4}$$

The symbol $m$ represents the molality of chloride and of buffer acid and ions indicated in the subscripts; $K$ is the ionization constant; $z_i$ is the valence and $f_i$ is the activity coefficient of each ion indicated in subscripts; $\mu$ is the ionic strength;[1] $a_i$ is the "ionic size"; $\beta$ is an empirical term; and $R$, $T$, and $F$ have their usual significance. $E°$ is the standard potential for the reaction $\frac{1}{2}$ $H_2$(1 atm)+AgCl (solid) $=H^+ + Cl^- + Ag$ (solid), forming HCl at an activity ($fm$) of unity. The values of $E°$ at 20°, 25°, and 30° are taken as 0.22550, 0.22238, and 0.21911 volt, respectively [2, 6].

For monobasic acid buffers, the last term of eq 2 is very small. For such buffers the parameters $a_i$ and $\beta$ of eq 3 must be evaluated from differences between several series of measurements of solutions with varying ratios of chloride ion to buffer acid and anion.

It may be emphasized that by means of precise work it is comparatively easy to obtain the p$K$ value of the buffer acid within $\pm 0.001$. The use of p$K$ in eq 4 to obtain the true pH of the buffer acid-salt mixture may, however, involve comparatively large uncertainties. The procedure of computing the pH value involves either the substitution in eq 1 of values of $f_i$ (from eq 3) or substitution in eq 4 of values of $f_i$ and of p$K$ (from eq 2). The best values of $a_i$ and $\beta$ (eq 3) for computing $f_i$ for the mixtures are obtained from the observed change of the last term of eq 2 when the buffer is diluted. When $a_i$ and $\beta$ values for the buffers have been ascertained from electromotive-force measurements of the solutions at several concentrations, the pH value may be computed with a high degree of certainty. Thus the pH values for the phthalate buffers, the malonate buffers, and the disodium-phosphate–dihydrogen-phosphate mixtures (solutions 3 to 11, inclusive) listed in table 1 are thought to be correct to well within 0.005 unit, for extensive measurements of these particular buffer mixtures have been made over wide ranges of temperature and concentration in the determination of the p$K$ values of the buffer acid by means of eq 2. The $a_i$ and $\beta$ values so obtained, however, apply only to the individual ions which compose the mixture and probably do not form a very sound basis for estimating the activity coefficients of mixtures of other salts of the buffer acid and other chlorides.

The pH values of the borate and phenolsulfonate buffers and of phosphate solutions 1, 2, 16, and 17 were derived from electromotive-force measurements without the use of the most precise $a_i$ and $\beta$ values for the mixtures themselves. Since the total activity-coefficient contribution (last term of eq 4) for these dilute buffers is of the order of 0.09 unit or less, an uncertainty of not over $\pm 0.02$ can safely be ascribed to the salt-effect term in the values listed.

A plot of the known buffer concentrations against the left side of eq 2, involving the measured electromotive-force data for a series of dilutions of a stock buffer-chloride solution of known ratio $m_{Cl}:m_{An}:m_{HAn}$, gives $-\log K$ (p$K$) at the extrapolated zero concentration of the buffer. This is true because the right-hand term, $-\log (f_{Cl} f_{HAn}/f_{An})$, becomes zero at the extrapolated zero concentration of the buffer-chloride mixture, in which all of the activity coefficients ($f_i$) are unity. The same limiting value of p$K$ is reached as a convergence point when any reasonable individual values of $a_i$ and $\beta$ are used in

[1] The ionic strength, $\mu$, is defined by $\mu = \Sigma m_i z_i^2/2$. For the computation of the molality of each ion species, strong electrolytes are considered to be completely ionized. The ionization of the weak acid is computed from the ionization constant of eq 2 and 4.

eq 3 for computing $\log f_i$ for each ion. These plots may, however, have widely different slopes, both negative and positive, when different values of $a_i$ and $\beta$ are chosen. It is possible then to choose values of $a_i$ and $\beta$ to keep p$K$ in eq 2 constant for all concentrations of the buffer [2]. With these "best" values for $a_i$, $\beta$, and p$K$, it is then possible to compute the pH value within the experimental error of 0.001 to 0.002 unit for any concentration of the buffer-chloride mixture at the same buffer ratio. As the sodium, potassium, and other salts in identical concentrations give slightly different electromotive-force data and may require different $a_i$ and $\beta$ values, it is obvious that much work, on all kinds of salts of the same buffer and on their mixtures with various chlorides and other salts, will be required before $a_i$ values for particular combinations of ions can be estimated to cover all buffer-salt mixtures. It is hoped that the activities of the buffers may also be measured by other more direct methods to obtain $a_i$ and $\beta$ values.

All of the pH values of table 1 are to be considered provisional. Further work on phthalate, phosphate, borate, and phenolsulfonate buffers is in progress and will be reported in detail at its completion.

## V. REFERENCES

[1] W. J. Hamer and S. F. Acree, J. Research NBS **23,** 647 (1939) RP1261.
[2] W. J. Hamer, J. O. Burton, and S. F. Acree, J. Research NBS **24,** 269 (1940) RP1284.
[3] D. I. Hitchcock and A. C. Taylor, J. Am. Chem. Soc. **59,** 1812 (1937).
[4] D. A. MacInnes, D. Belcher, and T. Shedlovsky, J. Am. Chem. Soc. **60,** 1094 (1938).
[5] W. J. Hamer, Trans. Electrochem. Soc. **72,** 257 (1937).
[6] H. S. Harned and R. W. Ehlers, J. Am. Chem. Soc. **54,** 1350 (1932); **55,** 652, 2179 (1933).

WASHINGTON, June 30, 1942.

U. S. DEPARTMENT OF COMMERCE NATIONAL BUREAU OF STANDARDS

RESEARCH PAPER RP1496

*Part of Journal of Research of the National Bureau of Standards, Volume 29, September 1942*

# SURFACE AVAILABLE TO NITROGEN ON BONE BLACK AND OTHER CARBONACEOUS ADSORBENTS[1,2]

By Victor R. Deitz[3] and Leland F. Gleysteen[3]

ABSTRACT

The adsorption of nitrogen was determined at liquid nitrogen and liquid oxygen temperatures by measuring the pressure decrease of a known volume of the gas exposed to each of 20 different samples of bone blacks, activated carbons, vegetable carbons, and coconut charcoals. Typical adsorption isotherms of these data are illustrated. Specific surfaces were estimated with fair accuracy from an analysis of the data with the aid of the multimolecular theory of adsorption. The surfaces of new bone chars, service bone chars, and spent bone chars are compared; the ratio of the specific surface of a new char to that of a spent char may be as great as 7. The distribution of pore sizes in the adsorbents is discussed and the data are divided into five groups, each characterized by a value of $n$, which is defined as the maximum number of adsorbed layers possible on the surface of the material. All the samples in each group have a common isotherm when reduced to unit surface. The differential heats of adsorption are also determined from the data. The adsorption at 77°K is also considered from the standpoint of capillary condensation. The volume, as adsorbed liquid nitrogen, is plotted against the corresponding radius of a cylindrical capillary, which is determined from the Kelvin equation.

CONTENTS

| | Page |
|---|---|
| I. Introduction | 191 |
| II. Adsorption experiments | 193 |
| 1. Surface area from adsorption measurements | 193 |
| 2. Apparatus | 194 |
| 3. Procedure | 195 |
| 4. Discussion of adsorption isotherms | 197 |
| III. Method of calculating the available surface | 202 |
| 1. Theoretical basis | 202 |
| 2. Discussion of table of results | 208 |
| IV. Isotherms reduced to unit surface | 211 |
| V. Heats of adsorption | 219 |
| VI. Dependence of the adsorption on capillarity | 221 |
| VII. References | 225 |

## I. INTRODUCTION

The filtration of sugar liquors through bone black has been a part of the procedure for cane-sugar purification for over a century. The technical application of this process has reached a relatively high state

[1] This investigation has resulted from a joint Research Project undertaken by the United States Cane Sugar Refiners and the bone char manufacturers and the National Bureau of Standards.

[2] A part of the material given in this paper was presented before the Division of Sugar Chemistry and Technology of the American Chemical Society at the Memphis meeting, April 1942.

[3] Research Associate at the National Bureau of Standards, representing the United States Cane Sugar Refiners and the bone black manufacturers.

of development without a corresponding advance in knowledge of the fundamental scientific principles involved. This situation is clearly reflected in the abundance of the patent literature on bone char as compared with purely scientific contributions. In realization of these conditions a joint research project has been undertaken by the United States Cane Sugar Refiners, the bone-black manufacturers, and the National Bureau of Standards. The object of this investigation is to study the fundamental physical and chemical principles which lead to the decolorization and purification of sugar liquors by bone char and analogous materials.

A vast scientific literature has accumulated on the general subject of carbonaceous and noncarbonaceous adsorbents. This includes investigations of their nature, preparation, and activation, of their use in gas adsorption and adsorption in liquids, and upon their use as catalysts. There are numerous applications of carbons to a variety of processes, such as the purification of sugar, foods, and medicines; the treatment of water and sewage; and refining of petroleum products; the recovery of solvents and gases; and, of timely interest, for protection against toxic gases. There will be no attempt in this report to cover the available literature. Reference is made, however, to the extensive bibliography which has been prepared in connection with this project for the period 1900–41, inclusive, on the general subject of adsorption from the gas phase and from solution, which is expected to be available in printed form at an early date.

One characteristic of all activated carbons and similar adsorbents is the large specific surface area which is attributed to them from many kinds of data. Estimates range from a thousand to a million times that of the external geometrical area as determined microscopically. This would include the surface bounding the cracks, pores, crevices, and channels, or whatever be the particular disposition of the interstices of the adsorbent. The chemist is, of course, interested in all regions to which a gas or solution may have access and hence be available for possible surface reaction. Consequently the primary problem is to obtain a fairly accurate measure of the total surface of the adsorbents with the object of studying the availability of this surface to gas molecules having various chemical and physical properties, and second, to study that part of the surface accessible to solution phenomena.

Many methods have been proposed to measure surface areas. Among these may be mentioned first the direct observation of the shape and dimensions of particles with a microscope, a method of obviously limited scope in adsorbents with large internal surfaces. The adsorption of radioactive indicators and the adsorption of dyes have been widely used since being introduced by Paneth [1].[4] Other methods that may be mentioned are the rate of chemical attack, which has been employed by comparison with a similar material of known surface area; the polarization during electrolysis on metal surfaces, which involves the use of the hydrogen ion in determining the extent of surface; the interference colors produced on metal surfaces, and the heat of wetting have also found application. The permeability method, which is concerned with the rate of flow of a fluid through a bed of material, has been applied by Carman [2] to evaluate the sur-

[4] Figures in brackets indicate the literature references at the end of this paper.

face areas of powders. Recently Kistler [3] has used the heat conductivity of a porous substance to estimate surface area.

Objections can be raised to any of the above methods on grounds of either their inapplicability to the present materials or their inadequate fundamental interpretation. There is described in this paper a method which seems to be less open to criticism, namely the measurement of the adsorption isotherm at low temperatures. Such data were obtained for 20 different materials at both liquid oxygen and liquid nitrogen temperatures, and the surface areas were calculated from these data.

## II. ADSORPTION EXPERIMENTS

### 1. SURFACE AREA FROM ADSORPTION MEASUREMENTS

The extent to which a solid is exposed to the action of a gas or liquid is generally much greater than the visible apparent surface. Obviously a large part of a porous structure is permeated only by small gas molecules, and it is such minute units that must serve as a measuring standard if the total surface is to be measured. Since molecular species vary in size and other properties, this qualification must be placed in the definition of the surface so measured. For example, the present investigation is a measurement of the surface *available to nitrogen molecules*.

When a gas or vapor is admitted to a thoroughly evacuated adsorbent, the molecules of the former distribute themselves between the gas phase and the adsorbed phase. The particular adsorption phenomenon in the neighborhood of the saturation point of the gas, generally termed van der Waals' adsorption, is usually identified with weak forces of interaction between the solid and the gas, similar to forces active in condensation phenomena. The characteristics of this type of adsorption are (1) the rapid attainment of an equilibrium state, and (2) the nonspecific nature of the adsorption. In contrast to this type is the so-called chemisorption in which the forces of interaction are strong, specific, and exhibit a similarity to the forces active in chemical reactions. Van der Waals' adsorption is free of chemisorptive effects except insofar as local regions modify the early stages in the formation of the first adsorbed layer.

The technique of measuring adsorption isotherms at low temperatures has been recently applied by Emmett and Brunauer [4] in determining the surface area of iron catalysts for synthetic ammonia. In a later paper by Brunauer and Emmett [5] the same method was used to determine the surface areas of a variety of adsorbents, including two charcoal samples. Finally Brunauer, Emmett, and Teller [6] derived isotherm equations for multimolecular adsorption which have proved to be of some generality. The application of this theory to bone char and to other adsorbents containing carbon is discussed in section IV of this paper, in connection with the measurement of nitrogen isotherms.

While the present paper was in preparation, three applications of this method have been published for a number of finely divided pigments and carbon blacks. It has been shown from electron-microscope pictures that carbon-black particles are approximately spherical, and an average value for the diameter is so obtained. This has been compared by Emmett and De Witt [7] with their value obtained from

a determination of the surface area by adsorption of nitrogen at 77° K. Excellent agreement was obtained: the particular carbon-black particles yielded a value of 280 A from electron-microscope data as compared with 310 A obtained from the nitrogen adsorption. Even more striking confirmation was found by Smith, Thornhill, and Bray [8], who compared the results for two samples of carbon black. Their acetylene-black sample showed a surface of 64 $m^2/g$ by adsorption of nitrogen, or an average particle diameter of 533 A; the electron microscope value was 510 A. Another sample of standard-grade rubber black (their number 6) showed a surface of 114 $m^2/g$ corresponding to a particle diameter of 284 A; the electron microscope value was 280 A. P. H. Emmett [14] recorded still another case for acetylene-black particles, the diameter of which was 520 A as determined from adsorption of nitrogen and 510 A as obtained with the electron microscope.

## 2. APPARATUS

The experiments to be described involve simply a determination of the pressure of nitrogen in a known volume over the adsorbent in the range of 1 to 760 mm of mercury after the introduction of a known quantity of the gas. The outline of the apparatus is shown in figure 1. With the exception of the pumps, gages, and other accessories, the apparatus consists of two sections: (1) the gas burette, manometer, and connecting capillary tubing up to stopcocks 2 and 3; and (2) the adsorption cell and the capillary tubing up to stopcocks 1 and 3, including the bore of stopcock 3. The gas burette, surrounded by a water jacket, was calibrated before assembling the apparatus by finding the weight of mercury required to fill each bulb. The mercury column in the manometer is about 1 cm in diameter. Behind the manometer is a mirrored meter scale, and the position of the mercury meniscus is noted when it is in coincidence with its image. The important stopcocks have hollow-stopper plugs with oblique bore, and were specially ground. The inside diameter of the capillary tubing was about 1 mm.

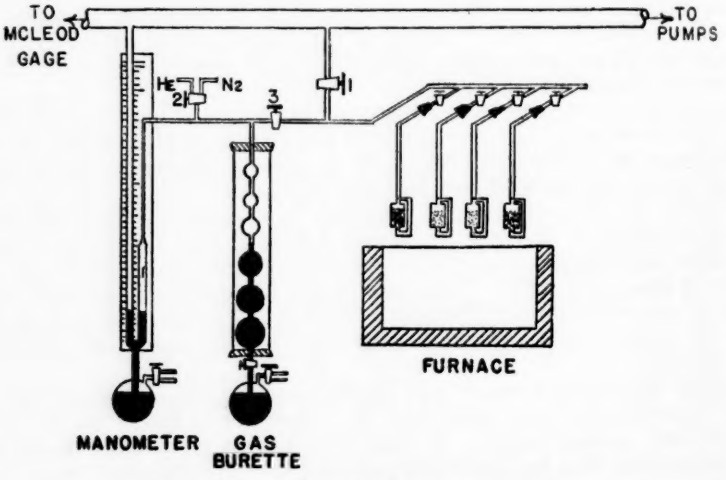


FIGURE 1.—*Adsorption apparatus for gases.*

The tube which contains the sample of adsorbent is shown in figure 2. Attention is directed to three features of construction: (1) The adsorbent is evacuated from above and from beneath, which, coupled with slow initial evacuation, is necessary to keep the sample in place; (2) the adsorbent sample, when placed beneath the surface of the cooling liquid, is really at the temperature of the liquid, since there is no opportunity for heat conduction through the connecting tubing to the sample; (3) the additional U-bend protects the adsorbent from stopcock grease and mercury vapor during the determination. After a known weight of sample is introduced through the side arm, it is sealed and the tube is attached to the main apparatus through a small ground-glass joint with a plastic cement.

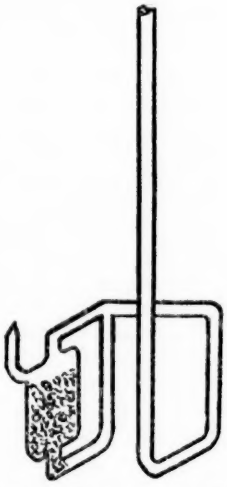

FIGURE 2.—*Special tube for the adsorbent in the adsorption of gases.*

With the use of the manifold system shown in figure 1, it is possible to run four different samples in sequence. The space around the sample of adsorbent and in the connecting capillary tubing is termed the "dead-space" of the apparatus. Its volume must of course be known in order to calculate the volume of gaseous nitrogen over the adsorbent at each pressure. This has been done under the same conditions as in the adsorption experiments by calibration with a known volume of purified helium. Helium is not appreciably adsorbed at the temperatures employed, and it is readily removed by pumping, with the adsorbent kept at room temperature.

### 3. PROCEDURE

The weight of the sample of adsorbent varied between 0.25 and 1.0 g. Except for samples 19 and 20, which are powdered materials, the particle sizes were between 35 and 80 mesh. The preparation of these samples and the analysis for carbon and hydrogen have been described [10].

474862—42——2

The samples of adsorbents contained in weighing tubes were dried in an air oven at 130° C for about 20 hours and were cooled in a desiccator. The weight was determined before and after the delivery of the sample into the adsorption tube, the transfer being accomplished as rapidly as possible.[5]

The four samples were simultaneously evacuated and heated according to a prescribed procedure. A mercury-diffusion pump supported by a Hyvac pump maintained a pressure of about $10^{-5}$ mm for periods of evacuation which lasted 18 to 24 hours. The temperature of outgassing could be varied up to 900° C, but in the experiments reported in this paper the temperature was between 300° and 400° C for all the materials. The continued outgassing of the samples between 300° and 400° C for periods longer than 18 to 24 hours had no influence on the nitrogen isotherm obtained. At higher temperatures significant changes do occur, and these will be reported in a future publication.

Following the outgassing period, stopcocks 1 and 3 were closed and the adsorbent was allowed to cool to room temperature. Helium was slowly admitted to the burette section of the apparatus through a charcoal trap immersed in liquid air. The pressure and the volume were noted. The bath to be used was raised into position around the adsorption bulb (either liquid oxygen, −183° C; or liquid nitrogen, −195.8° C). The known volume of helium was expanded onto the evacuated sample by opening stopcock 3 and the pressure then noted for given positions of the mercury in the burette. The temperature of the bath was determined with a calibrated copper-constantan thermocouple. The char was then allowed to warm to room temperature, and the helium was removed by pumping to a pressure (as read with a McLeod gage) of $10^{-5}$ mm of mercury. After this pumping, stopcocks 1 and 3 were closed and the bath was again placed in position around the adsorbent. The helium calibration was sometimes performed after the nitrogen isotherm had been determined and after the sample had been outgassed for several hours. The results were exactly the same, which indicates that the removal of helium by pumping at room temperature is essentially complete as far as this type of measurement is concerned.

Purified nitrogen was introduced into the first section with stopcock 3 closed. After the pressure was measured for a given setting of the level of mercury in the burette, the nitrogen was introduced into the evacuated sample. For values less than about 0.6 of the relative pressure, which is defined as the ratio of the pressure of the gas to the saturation pressure, a steady state was obtained in 15 to 20 minutes; at higher relative pressures a period of as much as an hour was sometimes necessary. Both adsorption and desorption points were obtained in order to detect possible hysteresis.

Liquid oxygen or liquid nitrogen was prepared from tank oxygen or tank nitrogen by passing the gas under pressure through a copper coil immersed in liquid air. The temperature of the liquid air determines the pressure necessary for liquefaction. This apparatus

[5] The weight of adsorbent need be known only to about 0.5 percent. Consequently the relatively elaborate method of drying discussed in [10] is not required.

has been described by Lane and Watson [9]. During the adsorption experiments, the bath was maintained at a constant level by additions from a reservoir of liquid nitrogen or liquid oxygen.

The nitrogen for the adsorption measurements was the commercial water-pumped product, which was purified by passage through a tube packed with metallic copper maintained at about 450° C. The gas then passed in order through Ascarite, activated alumina, and phosphorus pentoxide. It was drawn into the adsorption burette as required, and the excess was allowed to bubble through a mercury trap into the atmosphere.

## 4. DISCUSSION OF ADSORPTION ISOTHERMS

Isotherms for 20 different samples are reported. These include four samples of new, that is unused, bone char from different sources;

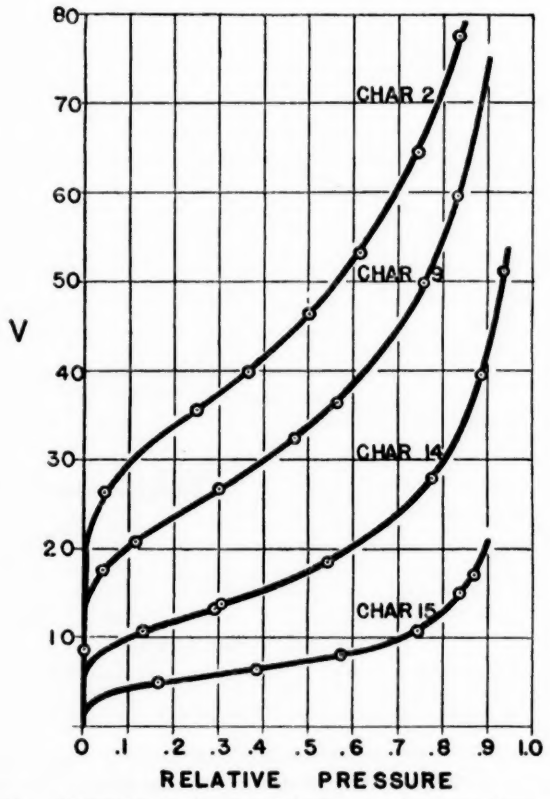


FIGURE 3.—*Adsorption isotherms of nitrogen on four bone chars at 77° K.*

The volume adsorbed, *V*, is in milliliters per gram of adsorbent.

six bone chars obtained from several cane-sugar refineries, where they were sampled at various stages in the char filtration; six decolorizing carbons other than bone char; two activated coconut-shell charcoals;

and, in order to broaden the scope of materials investigated, a sample of carbon black used in rubber compounding and a sample of petroleum coke. As mentioned before, these samples are the identical materials, and are numbered the same, as those previously described [10].

Altogether 57 nitrogen isotherms are considered in this paper for these 20 samples. Figures 3, 4, 5, 6, 7, and 8 are typical. Figure 3 illustrates the isotherms for four bone chars at 77° K. The coordinates are: relative pressure, $x$, as abscissa, $x$ being equal to the

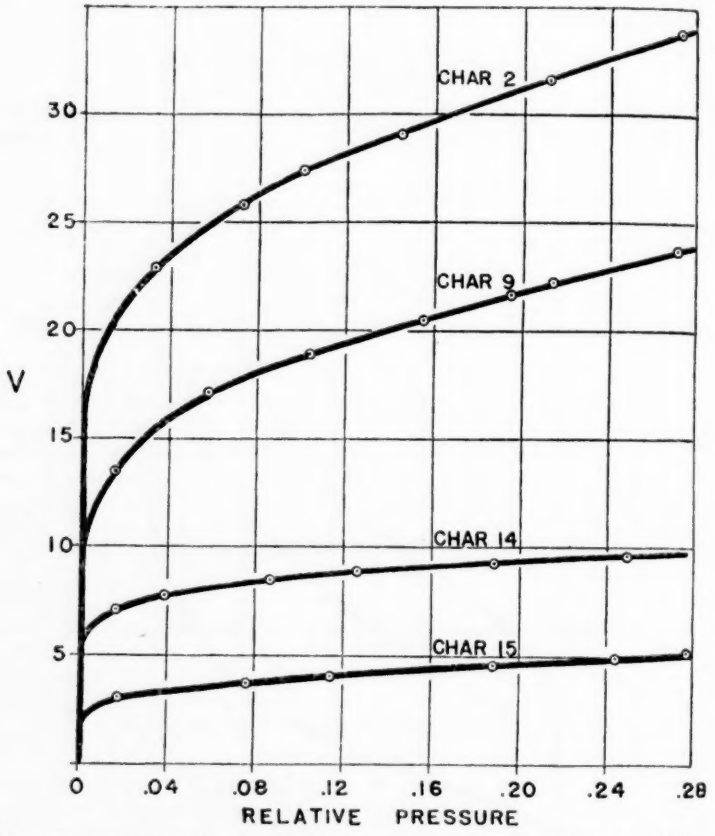


FIGURE 4.—*Adsorption isotherms of nitrogen on four bone chars at 90° K.*

The volume adsorbed, $V$, is in milliliters per gram of adsorbent.

pressure of nitrogen over the char divided by the vapor pressure of nitrogen at the particular temperature of the bath; the volume of nitrogen absorbed per gram, $V$, as ordinate, where the volume has been calculated to the standard conditions of 0° C and 760-mm pressure. The curve, char 2, is for a new sample of bone char; the two next curves, chars 9 and 14, are for service chars, of which char 9 had been in use for the shorter time; the bottom curve, char 15, is for a spent bone char.

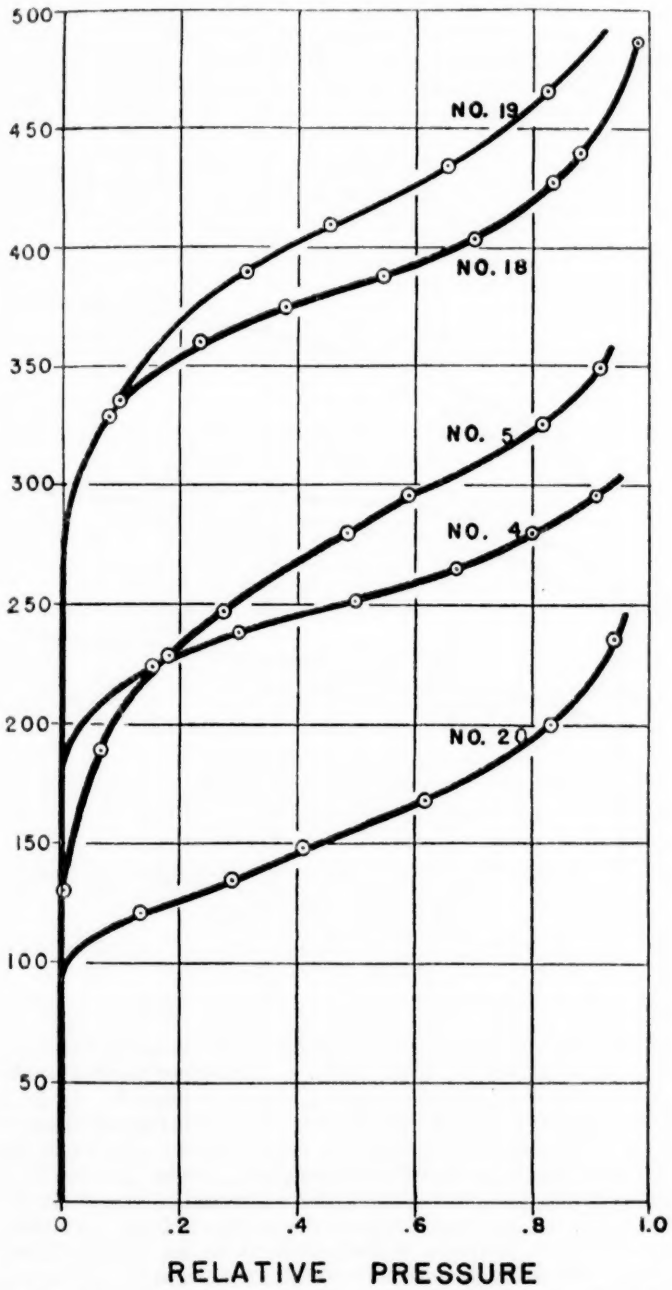


FIGURE 5.—*Adsorption isotherms of nitrogen on five adsorbent carbons other than bone char at 77° K.*

The volume adsorbed, *V*, is in milliliters per gram of adsorbent.

Figure 4 gives the isotherms for the same samples at 90° K. At first glance these curves might appear to be isotherms of the Langmuir type, where a limiting value of the adsorption is inferred. However further consideration shows that the curves are the first parts of S-shaped isotherms, which is to be expected in the relative pressure range up to $x=0.3$.

Figures 5 and 6 give the isotherms at 77° and 90° K, respectively, for a number of carbons other than bone char. It may be seen that the S-shaped isotherms of figure 5 are characteristic for these ma-

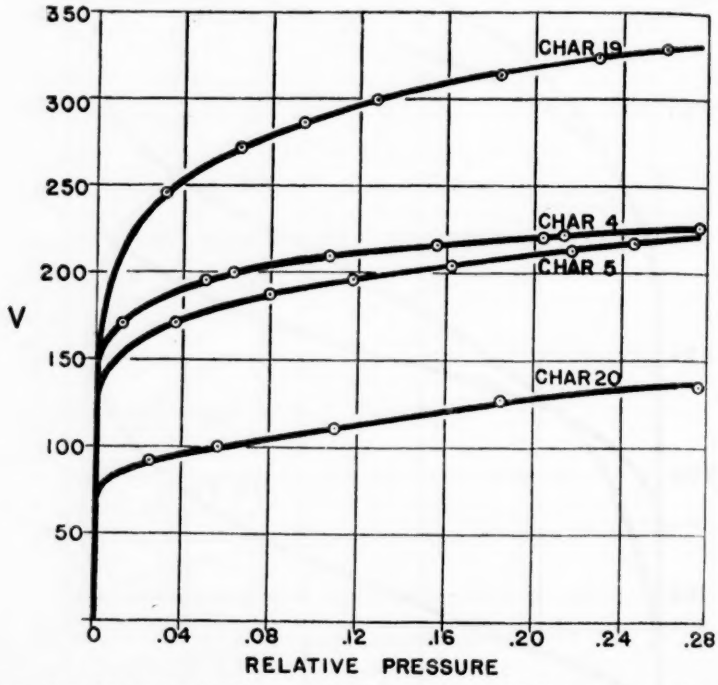


FIGURE 6.—*Adsorption isotherms of nitrogen on four adsorbent carbons other than bone char at 90° K.*

The volume adsorbed, $V$, is in milliliters per gram of adsorbent.

terials as well as for the bone chars of figure 3, although the volume of the nitrogen adsorbed is much larger. The experimental isotherm for the carbon-black sample in figure 7 is also S-shaped. In marked contrast to these isotherms is that for coconut-shell charcoal illustrated in figure 8. The adsorption here proceeds according to the Langmuir isotherm for unimolecular adsorption. Only at the highest pressure measured (above $x=0.9$) is there any indication of the curve turning upward. That gases are adsorbed on carbons according to the unimolecular mechanism is thus seen to be an exception rather than a rule. Of all the carbon adsorbents investigated in this paper, coconut-shell charcoal alone shows this property.

It is important to note that no pronounced hysteresis was detected in these experiments. Upon several occasions desorption points taken directly after the greatest pressure reading of the experiment were in complete agreement with the adsorption points.

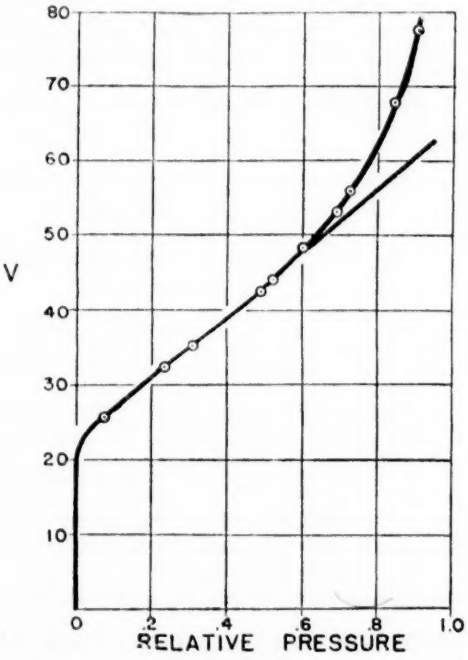


FIGURE 7.—*Observed and calculated isotherms of nitrogen on Arrow carbon black at 77° K.*

Experimental points are in circles, and the curve is calculated with $n=4$. The volume absorbed, $V$, is in milliliters per gram of absorbent. It is to be noted that as saturation is approached, $n$ most probably increases.

It may be seen that the isotherms at 90°K (figs. 4 and 6) extend about one-third toward saturation pressure and, therefore, are to be compared with the first third of the curves at 77°K (figs. 3 and 5). The curves in figure 6 also appear to be of the Langmuir type, but are merely the first portions of the S-shaped curves. Readings in the neighborhood of saturation are difficult because of the sensitivity of adsorption to small changes in pressure and temperature and the danger of condensation as the gas at a higher pressure is introduced to the adsorbent. It is to be further noted that the adsorption of carbon 19, which has an S-shaped curve, is greater in general than that of the coconut-shell charcoal 1, which is shown to follow a unimolecular isotherm, although, as will be shown later, the surface is greater for the coconut charcoal.

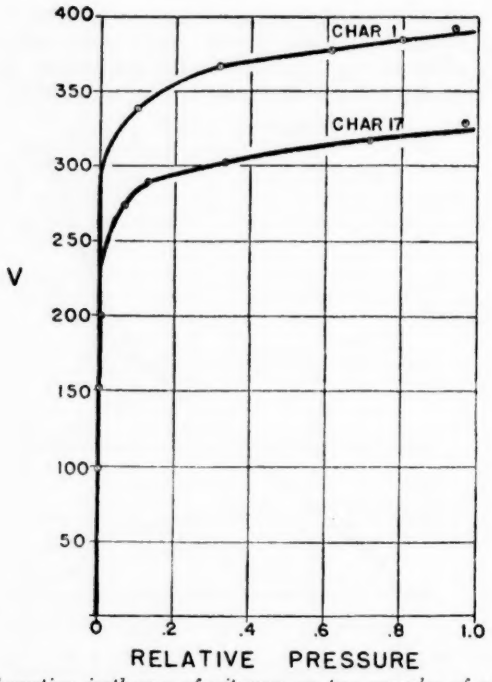


FIGURE 8.—*Adsorption isotherms of nitrogen on two samples of activated coconut-shell charcoals at 77° K.*

The volume adsorbed, $V$, is in milliliters per gram of adsorbent.

## III. METHOD OF CALCULATING THE AVAILABLE SURFACE

### 1. THEORETICAL BASIS

Brunauer, Emmett, and Teller [6] have developed a theory to account for the adsorption of gases in multimolecular layers. The development is a generalization of Langmuir's treatment of the unimolecular layer [11], and the theory is quantitative with certain limitations. According to these authors a statistical equilibrium exists between the formation of various layers due to condensation of the gas and the removal of the layers due to evaporation. By equating the rate of condensation of gas molecules on top of the $i$ th layer to the rate of evaporation from the $(i+1)$ th layer, an expression is derived which can be summed over the entire surface. The principal assumptions of this theory may be listed as follows: (1) the postulates of Langmuir as to the expressions for the rates of adsorption and evaporation; (2) the heat of adsorption in a given layer is independent of the number of adsorbed molecules already present; (3) the heats of adsorption in the second, third, and higher layers are equal to each other and to the heat of liquefaction ($E_L$); (4) the ratio of the rate constant for evaporation to the rate constant for condensation is the

same in the second and higher layers; (5) the heat of adsorption in the first layer, $E_1$, may be estimated if the ratio of the rate constants in the first layer is assumed to be the same as in higher layers. These assumptions limit the pressure range to which the theory can be applied. It may not be applicable to relative pressures less than about 0.05, since local enhanced heats of adsorption may lead to chemisorptive processes. Also at the higher relative pressures approaching saturation, the interactions of neighboring molecules within the layer become significant and may lead to deviations.

Three equations are developed in [6] which have application to the data of this paper:

$$V=\frac{v_m cx}{1-x}\left[\frac{1-(n+1)x^n+nx^{n+1}}{1+(c-1)x-cx^{n+1}}\right] \tag{1}$$

$$V=\frac{v_m cx}{1+cx} \qquad \text{or} \qquad \frac{p}{V}=\frac{p_0}{cv_m}+\frac{p}{v_m} \tag{2}$$

$$V=\frac{v_m cx}{1-x}\left[\frac{1}{1-x+cx}\right] \qquad \text{or} \qquad \frac{p}{V(p_0-p)}=\frac{1}{v_m c}+\left[\frac{c-1}{v_m c}\right]\frac{p}{p_0} \tag{3}$$

$V$ = the volume of gas at 0° and 760 mm adsorbed per gram.

$v_m$ = the volume of gas at 0° and 760 mm which, when adsorbed, covers the surface of 1 g of the adsorbent with a unimolecular layer.

$p$ = the pressure.

$x$ = the relative pressure of the gas and is equal to $p/p_0$, where $p_0$ is the saturation pressure of the gas at the temperature of the adsorption.

$n$ = the maximum number of adsorbed layers to which the adsorption is limited in thickness.

$c$ = the measure of the increase of the heat of adsorption over the heat of liquefaction ($E_L$), namely, $E_1-E_L=2.303\ RT\ \log\ c$, where $E_1$ is the heat of adsorption in the first layer, $R$ is the gas constant in calories per mole per degree, and $T$ is the temperature in degrees K. Equation 1 was derived by summing the condensation-evaporation equilibria over the total surface with the provision that $n$ is finite. This factor, $n$, will be referred to in some detail in this paper.

Equations 2 and 3 are limiting cases of eq 1. When $n=1$, eq 1 reduces to the Langmuir-type eq 2, which accounts very well for the data obtained with the activated coconut-shell charcoals. From the second formulation of eq 2 a straight-line graph may be obtained by plotting $p/V$ against $p$, and the values of $v_m$ and $c$ may be calculated from the slope and intercept, respectively. Figure 9 illustrates the behavior of a sample of coconut-shell charcoal. The agreement with the required linearity is excellent.

In contrast to unimolecular adsorption, there is the opposite extreme of adsorption on open free surfaces where $n$ may be infinitely large, that is, where there is no limitation to the number of adsorbed layers that can form on the surface. In this case eq 1 reduces to eq 3. For values of $n$ as large as 4 or 5, which is the case for bone chars, and for values of $x$ up to 0.25, eq 3 becomes a good approximation to eq 1. Hence to use this approximation, one plots the experimental isotherm in the low-pressure region with $p/V(p_0-p)$ as ordinate and $x$ as

abscissa, according to the second formulation of eq 3, and from the intercept of the straight line, equal to $1/v_m c$, and its slope, equal to $(c-1)/v_m c$, it is possible to evaluate $c$ and $v_m$. In applying these equations to the bone-char data, such linear curves are obtained, as may be seen in figure 10. The data used are the same as those given in the isotherms of figure 4.

There is an alternative method of evaluating $v_m$ and $c$, which may be used for bone chars and which must be used in the case of decoloriz-

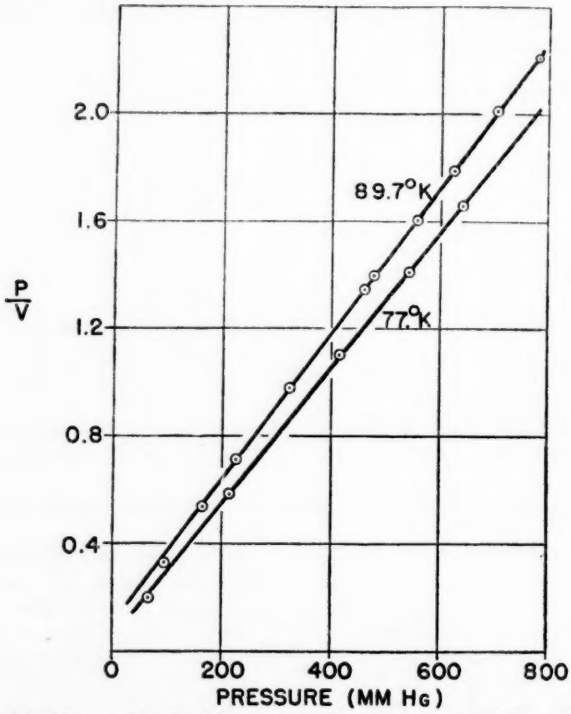


FIGURE 9.—*The linear plot of $p/V$ against $p$ for nitrogen adsorbed on No. 1 sample of coconut-shell charcoal at 89.7° and 77°K.*

Note that the maximum pressure for the 89.7°K line corresponds to a relative pressure of about 0.3, but the point at 650 mm on the 77°K line corresponds to a relative pressure of 0.85.

ing carbons other than bone char. This consists in substituting the experimental values of $V$ (for example at $x=0.1$ and 0.2) into eq 1. Upon assuming different values for $n$, the resulting calculated values for $v_m$ and $c$ are tested by comparing the remaining part of the adsorption isotherm with the experimental data. Figure 11 illustrates the results for new bone char 2 and figure 12 for service bone char 3. As may be seen from these plots, it is possible to reproduce the experimental isotherm for a particular set of constants up to a relative pressure of about 0.5 to 0.6. Above this pressure the observed adsorption always increases faster than the calculated values. The sets of values for $n$, $v_m$, and $c$ giving the best agreement are entered in table 1 and will be discussed in the next section.

For the decolorizing carbons other than bone char, the linear plot of $p/V(p_0-p)$ against $p/p_0$ does not hold as it did for the bone chars.

The plot of $p/V$ against $p$, which is the test for unimolecular adsorption, also is not linear. The explanation is that the values for $n$ are approximately 1.5 or 2 and for these small values eq 3 cannot hold. Consequently $v_m$ and $c$ must be calculated by substituting the experimental values of $V$ and $x$ into eq 1, assuming different values for $n$, in the manner described above. Figure 13 illustrates the results for carbon 6. When $n$ is assumed to be 1.5, the values obtained are $v_m=141$ and $c=58$; when $n=2$, $v_m=129$ and $c=106$; finally when $n=3$, $v_m=119$ and $c=510$. The value of $n=2$ yields a calculated curve which is in best agreement with experiment up to a relative pressure

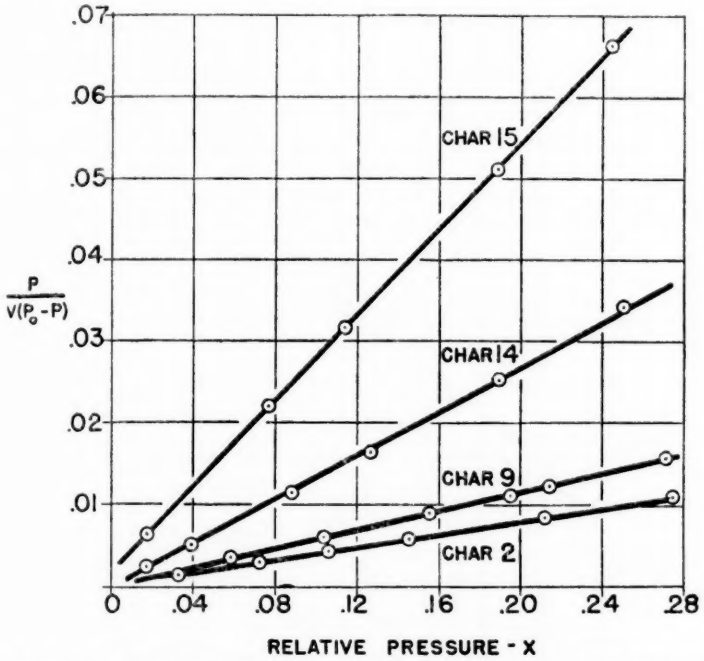


FIGURE 10.—*The linear plot of $p/V(p_0-p)$ against $p/p_0$ for nitrogen adsorbed on four samples of bone chars at 90° K.*

of about 0.4 to 0.5. A value of 2.2 would, perhaps, give a little better agreement; however, for the present no attempt has been made to establish the absolute value of $n$ with greater accuracy. A value of $n=2.2$ has been reported by Brunauer, Emmett, and Teller [6] for a sample of activated carbon designated as granular Darco G. In connection with this behavior, these authors [6] have pointed out that as long as the capillaries of an adsorbent are fairly uniform in diameter, eq 1 can describe the entire course of the isotherm with a fair degree of accuracy. Should the size of the pores in an adsorbent vary considerably from the average, the experimental points will fall above the theoretical curve at higher pressures and below the curve at lower pressures. They propose an equation to take care of the varying size of capillaries, but its practical use is inexpedient because of the large number of constants. The subject of capillaries is further discussed in section VII.

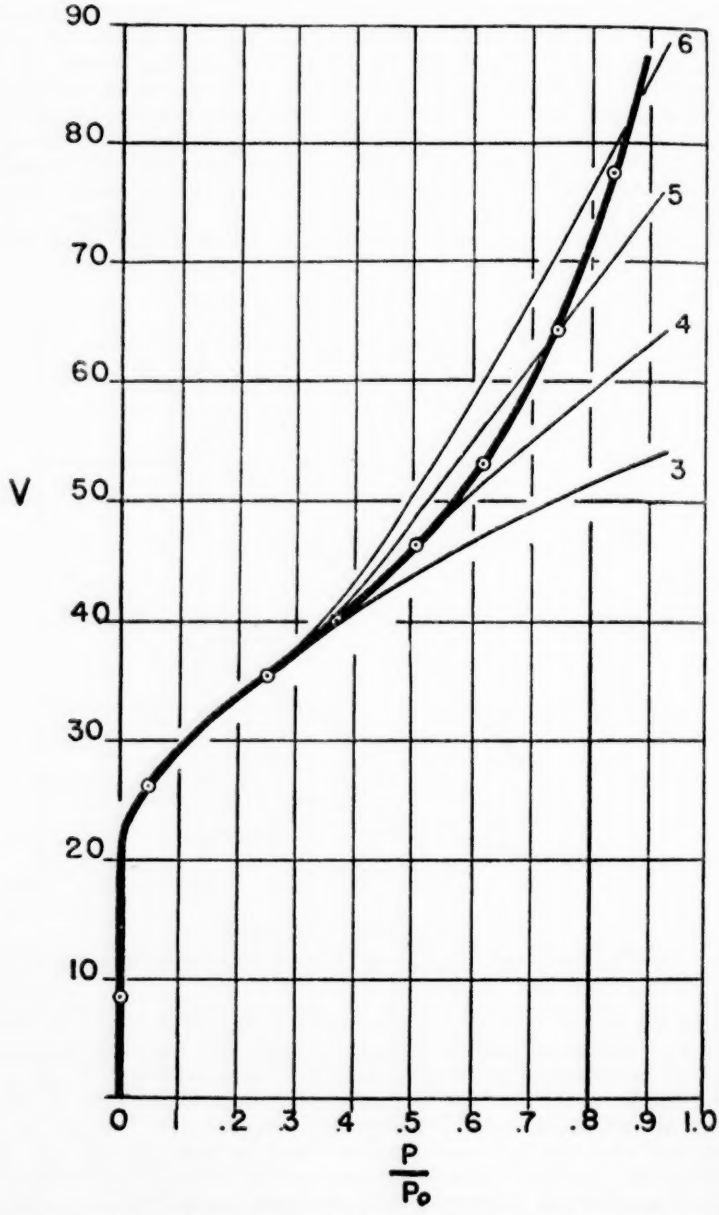


FIGURE 11.—*Observed and calculated isotherms of nitrogen adsorbed on new bone-char sample 2 at 77° K.*

Experimental points are in circles, and isotherms are calculated at values of $n=3$, 4, 5, and 6. The volume adsorbed, $V$, is expressed in milliliters per gram of adsorbent.

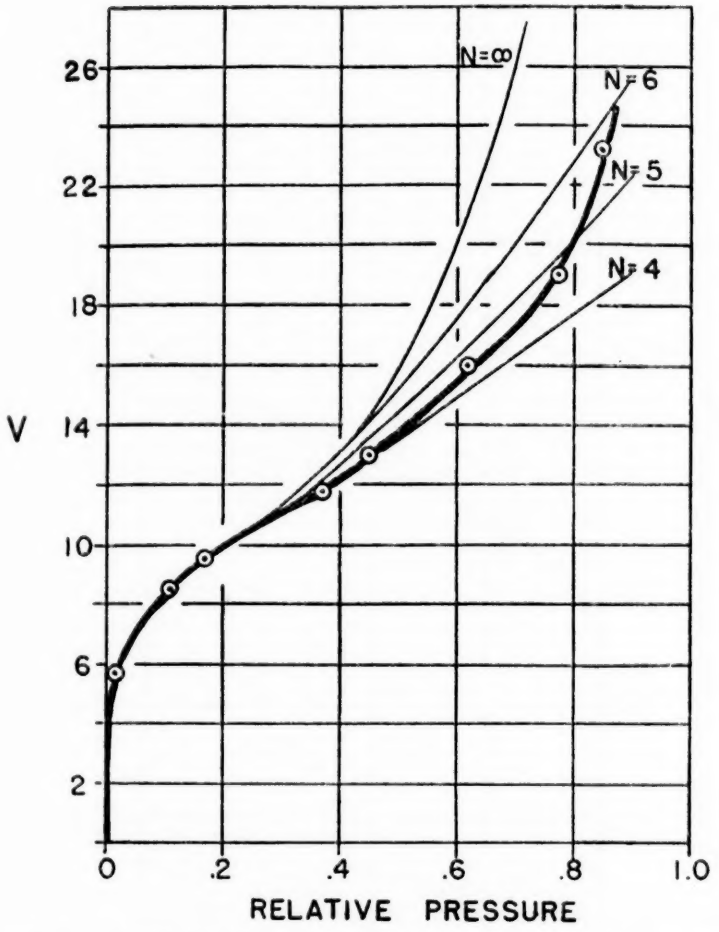


FIGURE 12.—*Observed and calculated isotherms of nitrogen adsorbed on service bone-char sample No. 3 at 77° K.*

Experimental points are in circles, and isotherms are calculated at values of $n=4$, 5, 6, and $\infty$. The volume adsorbed, $V$, is expressed in milliliters per gram of adsorbent.

It may be observed that the calculated isotherms are more sensitive to a unit change in $n$ when $n$ is small than when $n$ is large. This may be seen by comparing figures 11 and 13. It is surprising that the isotherms of a new bone black (fig. 11) and a service bone black (fig. 12) may be fitted by the same value of $n$. The progressive aging of a bone black, with its accompanying decrease in efficiency, has been attributed to the accumulation of insoluble salts. However, if this deposition occurred in the larger pores, the distribution of pore sizes in new and used bone-black samples would be essentially unchanged for gas adsorption.

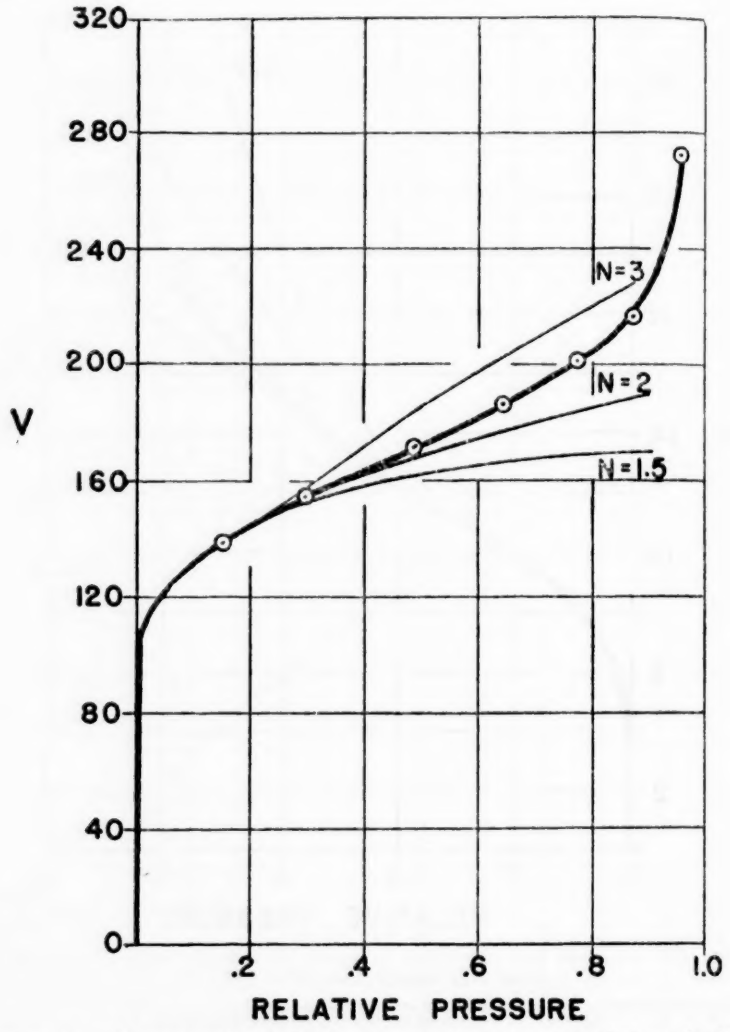


FIGURE 13.—*Observed and calculated isotherms of nitrogen adsorbed on the No. 6 activated carbon at 77° K.*

Experimental points are in circles, and curves are calculated at values of $n=1.5$, 2, and 3. The volum adsorbed, $V$, is expressed in milliliters per g of adsorbent. For $n=1.5$, $v_m=141$, and $c=58$; when $n=2$, $v_m=129$, and $c=106$; when $n=3$, $v_m=119$, and $c=510$.

## 2. DISCUSSION OF TABLE OF RESULTS

Table 1 summarizes the results for the surface calculations. As previously mentioned, $v_m$ is the volume of nitrogen measured at 0° C and 760 mm which, when adsorbed, covers the surface of 1 g of sample with a unimolecular layer. The first group contains the data for new bone-char samples from different manufacturers. The values for $n$ are either 4 or 5. In the second group are the bone chars which have been in service in cane-sugar refineries, and for these, too, $n$ is either

4 or 5. The third group includes the vegetable and the activated carbons, and for these $n$ is either 1.5 or 2. The two charcoal samples in group 4 are definitely characterized by $n=1$. Finally, for the carbon black sample, $n$ is about 4, but for pressures higher than $x=0.6$, $n$ most probably increases.

In order to calculate the area of the surface from $v_m$, it is necessary to know how the nitrogen molecules are packed on the adsorbing surface, since its area is simply the product of the number of adsorbed molecules times the average area that each molecule occupies in the adsorbed state. This procedure has been discussed by Emmett and Brunauer [4] and by Brunauer, Emmett, and Teller [6], who considered liquidlike packing as the best approximation that is available at present. The uncertainty in the knowledge of the packing factor constitutes the main limitation on the accuracy of this method of surface measurement. For comparative purposes the error introduced by this uncertainty is cancelled. A rough estimate of the accuracy would indicate a value of 5 percent for relative purposes, usually much better, but about 20 percent for absolute accuracy. However, the agreement with the electron-microscope data for the carbon blacks, as mentioned in section II–1, indicates much better accuracy than 20 percent for particles which may be considered relatively nonporous. There is no method at present to check the surface calculations for highly porous materials. However, there does not appear to be any reason for assuming unique adsorption behavior for highly porous materials in the regions in which capillarity effects, such as hysteresis, are excluded.

By assuming hexagonal close-packing for liquid nitrogen, one obtains for the diameter, $D$, of a single $N_2$ molecule:

$$D^3=\frac{6v(0.74)}{N_A\pi},$$

where $v$ is the molar volume of the liquid in milliliters, $N_A$ is Avogadro's number, the factor 0.74 is the fraction of the total space filled by spheres hexagonally close-packed. Thus $D$ is the diameter in centimeters of an isolated sphere. When the surface is covered, hexagonal close-packing in two dimensions is assumed to occur, and in this case the fraction of the surface covered by the projection of the spheres on the surface is 0.908. The surface, $S$, in square meters, covered by 1 ml of gas becomes:

$$S=2.705\times10^{19}\left[\frac{1}{0.908}\right]\frac{\pi}{4}\left[\frac{6v(0.74)}{N_A\pi}\right]^{2/3}=0.412v^{2/3}.$$

$2.705\times10^{19}$ is the number of gas molecules per milliliter. The molar volume for liquid nitrogen was obtained from the International Critical Tables. A plot was made of $S$ against $T$ in order to facilitate the calculation for the surface of each sample at the particular temperature of the experiment. For example, at 90.0° K, $S=4.61_5$ m²/ml $N_2$, and at 77.0° K, $S=4.37_3$ m²/ml $N_2$.

The results of the surface calculation are shown in column 7 of table 1. The surfaces of new bone chars vary only from 104 to 120 m²/g for four samples of different manufacturers, a fact which is indicative of the uniformity of the current production of bone char. Bone char 9 of limited service shows a surface of 83.5; the char, 8,

of gray appearance is next with a surface of 60.2; three other service chars show surfaces of 40.1, 37.2, and 35.6; a spent char shows a surface of 18.0. We may therefore draw a parallel for these bone chars between the surface areas and the efficiencies with which the samples are known to decolorize sugar liquors. However, it should be pointed out at once that the surface available to nitrogen molecules is not that available for adsorption from solution. The ratios between the total surfaces of materials of similar origin may, nevertheless, be the same as the ratios of the corresponding surfaces available to solution adsorption.

It is to be noted that the wide spread in the values for $c$ in various experiments with the same char does not imply corresponding uncertainties in $E_1-E_L$. This is due to the logarithmic relationship $E_1-E_L=2.3\ \mathrm{RT}\log c$.

TABLE 1.—*Results of the surface calculations for bone chars and other carbonaceous adsorbents*

| Type of char | Experiment No. | Temperature | $n$ | $r_m$[1] | $S$ | $c$ |
|---|---|---|---|---|---|---|
| | | | GROUP I | | | |
| | | °K | | *ml at STP*[2] | *m²/g* | |
| New bone char 2 | 12–a | 76.4 | 4 | 27.2 | 119 | 208 |
| Do | 14–a | 76.3 | 4 | 27.6 | 120 | 487 |
| Do | 19–c | 90.0 | 4 | 25.4 | 117 | 216 |
| Do | 16–e | 89.9 | 4 | 26.0 | 120 | 202 |
| Do | 1 | 89.5 | 4 | 25.5 | 118 | 105 |
| Do | 12–e | 89.3 | 4 | 25.8 | 119 | 187 |
| New bone char *C* | 21–a | 77.3 | 5 | 24.6 | 108 | 138 |
| Do | 21–b | 90.1 | 5 | 22.6 | 104 | 163 |
| New bone char *B* | 21–a | 77.3 | 5 | 23.3 | 102 | 291 |
| Do | 21–b | 90.1 | 5 | 22.5 | 104 | 141 |
| New bone char 16 | 20–a | 77.2 | 5 | 23.9 | 104 | 466 |
| Do | 13 | 89.3 | 5 | 22.6 | 104 | 163 |
| Do | 20–j | 90.4 | 5 | 21.7 | 101 | 163 |
| | | | GROUP II | | | |
| Service bone char 3 | 12–a | 76.4 | 4 | 8.17 | 35.7 | 137 |
| Do | 14–a | 76.3 | 4 | 9.39 | 41.0 | 760 |
| Do | 16–e | 89.7 | 4 | 7.51 | 34.6 | 91 |
| Do | 19–c | 90.0 | 4 | 8.37 | 38.6 | 99 |
| Do | 12–e | 89.3 | 4 | 7.85 | 36.1 | 186 |
| Service bone char 8 (gray) | 17–l | 77.0 | 4 | 13.75 | 60.2 | 370 |
| Do | 17–a | 89.8 | 4 | 13.06 | 60.2 | 160 |
| Service bone char 9 | 17–l | 77.0 | 4 | 19.28 | 84.4 | 147 |
| Do | 17–a | 89.8 | 4 | 17.97 | 82.8 | 142 |
| Service bone char 14 | 17–l | 77.2 | 5 | 9.4 | 41.2 | 169 |
| Do | 17–a | 89.7 | 5 | 8.5 | 39.2 | 100 |
| Do | 8 | 89.5 | 5 | 8.51 | 39.2 | 95 |
| Do | 10 | 89.4 | 5 | 8.89 | 40.9 | 105 |
| Service char 12 | 22 | 77.8 | 4 | 8.55 | 37.5 | 200 |
| Do | 1 | 89.5 | 4 | 7.30 | 33.7 | 240 |
| Spent char 15 | 22 | 77.8 | 4 | 4.25 | 18.5 | 177 |
| Do | 10 | 89.4 | 4 | 3.82 | 17.6 | 115 |

[1] Adsorption per gram of adsorbent.
[2] Standard temperature and pressure.

TABLE 1.—*Results of the surface calculations for bone chars and other carbonaceous adsorbents*—Continued

| Type of char | Experiment No. | Temperature | $n$ | $v_m$[1] | $S$ | $c$ |
|---|---|---|---|---|---|---|
| | | | GROUP III | | | |
| | | °K | | *ml at STP*[2] | $m^2/g$ | |
| Vegetable carbon 4 | 15–a | 76.7 | 1.5 | 214 | 937 | 164 |
| Do | 15–i | 89.6 | 1.5 | 200 | 923 | 280 |
| Do | 18–d | 89.9 | 1.5 | 201 | 930 | 317 |
| Vegetable carbon 5 | 15–a | 76.7 | 2.0 | 210 | 925 | 100 |
| Do | 15–i | 89.6 | 2.0 | 180 | 830 | 184 |
| Do | 18–d | 89.9 | 2.0 | 184 | 852 | 207 |
| Activated carbon 6 | 15–a | 76.7 | 2.0 | 129 | 563 | 106 |
| Do | 15–i | 89.6 | 2.0 | 93 | 432 | 146 |
| Do | 18–d | 89.9 | 2.0 | 118 | 548 | 360 |
| Activated carbon 19 | 20–a | 77.3 | 2.0 | 305 | 1,340 | 200 |
| Do | 20–j | 90.4 | 2.0 | 279 | 1,290 | 165 |
| Activated carbon 20 | 20–a | 77.3 | 2.0 | 115 | 506 | 100 |
| Do | 20–j | 90.4 | 2.0 | 103 | 478 | 220 |
| Activated carbon 18 | 23 | 77.6 | 1.5 | 329 | 1,440 | 216 |
| Do | 11 | 89.3 | 1.5 | 300 | 1,380 | 178 |
| | | | GROUP IV | | | |
| Coconut charcoal 1 | 12–a | 76.4 | 1 | 425 | 1,860 | 25 |
| Do | 14–a | 76.3 | 1 | 430 | 1,880 | ..... |
| Do | 12–e | 89.3 | 1 | 364 | 1,675 | 64 |
| Do | 16–a | 89.6 | 1 | 367 | 1,690 | 70 |
| Do | 16–e | 89.7 | 1 | 370 | 1,700 | 72 |
| Do | 19–e | 90.0 | 1 | 377 | 1,730 | 83 |
| Coconut charcoal 17 | 24–b | 90.0 | 1 | 293 | 1,350 | 64 |
| Do | 24–e | 77.6 | 1 | 323 | 1,420 | 107 |
| | | | GROUP V | | | |
| Carbon black *A* | 24–a | 77.6 | 4 | 25.52 | 112 | 168 |
| Do | 24–b | 90.0 | 4 | 24.27 | 112 | 111 |
| Petroleum coke 13 | 23 | 77.6 | 2 | 0.12 | 0.53 | 100 |
| Do | 5 | 89.8 | ..... | .11 | .51 | ..... |

[1] Adsorption per gram of adsorbent.
[2] Standard temperature and pressure.

## IV. ISOTHERMS REDUCED TO UNIT SURFACE

The isotherms for the group of bone chars show wide variance in the amount of nitrogen adsorbed. By referring to figure 3 and to table 2, it may be seen that the volumes of nitrogen adsorbed at $x=0.2$, for example, are 33.4, 23.3, 11.7, and 5.13 ml for bone chars 2, 9, 14, and 15, respectively. The corresponding values for $v_m$, as given in table 1, may be seen to vary between 22.6 for char 2 and 4.25 for char 15, which is greater than a fivefold variation. Despite these large differences, it will be seen from the following calculation that the amount of nitrogen adsorbed per unit surface of each sample is the same for all the bone chars at a given relative pressure of the nitrogen. This is true to within the over-all error of the experiments at relative pressures from $x=0.1$ to $x=0.6$.

The data in table 2 illustrate this correlation for a number of bone chars at 77°K. The values for $V$ were obtained from the experimental isotherms for the given values of $x$. The definitions of $x$, $V$, and $v_m$ are as previously used. Figure 14 shows this same conclusion in a graphical manner, an average curve being drawn through the points indicated. At relative pressures of $x=0.6$ and higher, individual differences begin to be manifested. At higher pressures slight differences in the distribution of the wider pores bring about differences in the amount adsorbed. But below $x=0.6$ the quantity of nitrogen adsorbed (at a given value of $x$) depends simply on the area of the surface available to the nitrogen. As indicated in the tables, the total spread of the values for $V/v_m$ is rarely more than 5 percent.

TABLE 2.—*Value of $V/v_m$ for the adsorption of nitrogen on bone chars at 77° K*

[Values given under $V$ are in milliliters at STP]

| $x$ | New char 2 | | New char 2 | | Service char 9 | | Service char 8 (gray) | | Service char 3 | |
|---|---|---|---|---|---|---|---|---|---|---|
| | $V$ (obs.) | $V/v_m$ | $V$ (obs.) | $V/v_m$ | $V$ (obs.) | $V/v_m$ | $V$ (obs.) | $V/v_m$ | $V$ (obs.) | $V/v_m$ |
| 0.1 | 29.0 | 1.06 | 30.0 | 1.08 | 20.2 | 1.05 | 14.9 | 1.08 | 10.2 | 1.08 |
| 0.2 | 33.4 | 1.23 | 34.2 | 1.24 | 23.3 | 1.21 | 17.0 | 1.23 | 11.6 | 1.23 |
| 0.3 | 37.4 | 1.37 | 38.2 | 1.38 | 26.5 | 1.37 | 19.0 | 1.37 | 13.0 | 1.38 |
| 0.4 | 41.5 | 1.52 | 42.2 | 1.53 | 29.7 | 1.54 | 21.5 | 1.55 | 14.3 | 1.52 |
| 0.5 | 46.3 | 1.70 | 46.5 | 1.68 | 33.7 | 1.75 | 24.2 | 1.75 | 15.7 | 1.67 |
| 0.6 | 51.8 | 1.90 | 52.2 | 1.89 | 38.4 | 1.99 | 27.0 | 1.95 | 17.5 | 1.86 |
| 0.7 | 60.2 | 2.21 | 60.2 | 2.18 | 44.8 | 2.32 | 31.3 | 2.26 | 19.8 | 2.11 |
| | Exp. 12-a $n=4$ $v_m=27.24$ | | Exp. 14-a $n=4$ $v_m=27.60$ | | Exp. 17-1 $n=4$ $v_m=19.28$ | | Exp. 17-1 $n=4$ $v_m=13.8$ | | Exp. 14-a $n=4$ $v_m=9.39$ | |

| $x$ | Service char 14 | | Service char 12 | | Service char 3 | | Spent char 15 | | New char 16 | |
|---|---|---|---|---|---|---|---|---|---|---|
| | $V$ (obs.) | $V/v_m$ | $V$ (obs.) | $V/v_m$ | $V$ (obs.) | $V/v_m$ | $V$ (obs.) | $V/v_m$ | $V$ (obs.) | $V/v_m$ |
| 0.1 | 10.3 | 1.06 | 9.1 | 1.06 | 8.5 | 1.04 | 4.5 | 1.06 | 26.3 | 1.09 |
| 0.2 | 11.7 | 1.21 | 10.5 | 1.23 | 10.0 | 1.22 | 5.13 | 1.21 | 29.9 | 1.24 |
| 0.3 | 13.6 | 1.40 | 11.7 | 1.37 | 11.1 | 1.36 | 5.87 | 1.38 | 33.7 | 1.40 |
| 0.4 | 15.8 | 1.63 | 13.1 | 1.54 | 12.3 | 1.51 | 6.40 | 1.51 | 38.2 | 1.59 |
| 0.5 | 18.3 | 1.89 | 14.6 | 1.71 | 13.8 | 1.69 | 7.12 | 1.67 | 43.0 | 1.79 |
| 0.6 | 20.8 | 2.14 | 16.8 | 1.97 | 15.5 | 1.90 | 8.25 | 1.94 | 48.9 | 2.04 |
| 0.7 | 23.7 | 2.45 | 19.7 | 2.31 | 17.3 | 2.12 | 9.78 | 2.30 | 58.7 | 2.44 |
| | Exp. 17-1 $n=5$ $v_m=9.68$ | | Exp. 22 $n=4$ $v_m=8.53$ | | Exp. 12-a $n=4$ $v_m=8.17$ | | Exp. 22 $n=4$ $v_m=4.25$ | | Exp. 20-a $n=5$ $v_m=23.98$ | |

| $x$ | New char $C$ | | New char $B$ | | Spread of $V/v_m$ for $n=4$ | | | Spread of $V/v_m$ for $n=5$ | | |
|---|---|---|---|---|---|---|---|---|---|---|
| | $V$ (obs.) | $V/v_m$ | $V$ (obs.) | $V/v_m$ | Min. | Max. | Deviation | Min. | Max. | Deviation |
| | | | | | | | % | | | % |
| 0.1 | 25.7 | 1.05 | 25.0 | 1.07 | 1.04 | 1.08 | 4 | 1.05 | 1.09 | 4 |
| 0.2 | 29.8 | 1.21 | 28.7 | 1.23 | 1.21 | 1.24 | 3 | 1.21 | 1.24 | 3 |
| 0.3 | 34.3 | 1.39 | 32.6 | 1.40 | 1.37 | 1.40 | 2 | 1.39 | 1.40 | 1 |
| 0.4 | 39.0 | 1.58 | 37.1 | 1.59 | 1.51 | 1.55 | 3 | 1.58 | 1.63 | 4 |
| 0.5 | 44.1 | 1.80 | 42.0 | 1.80 | 1.67 | 1.75 | 4 | 1.79 | 1.89 | 5 |
| 0.6 | 50.2 | 2.04 | 48.0 | 2.06 | 1.86 | 1.99 | 6 | 2.04 | 2.14 | 5 |
| 0.7 | 58.6 | 2.39 | 56.8 | 2.44 | 2.11 | 2.32 | 9 | 2.39 | 2.45 | 3 |
| | Exp. 21 $n=5$ $v_m=24.55$ | | Exp. 21 $n=5$ $v_m=23.26$ | | | | | | | |

Table 3 contains the data for bone chars at liquid oxygen temperature; these data are shown graphically in figure 15. It may be of interest at this stage to point out the widely different sources of these samples. The new bone chars were obtained from three separate manufacturers. Service char 9 was furnished by the National Sugar Refining Company. It had been used about a month

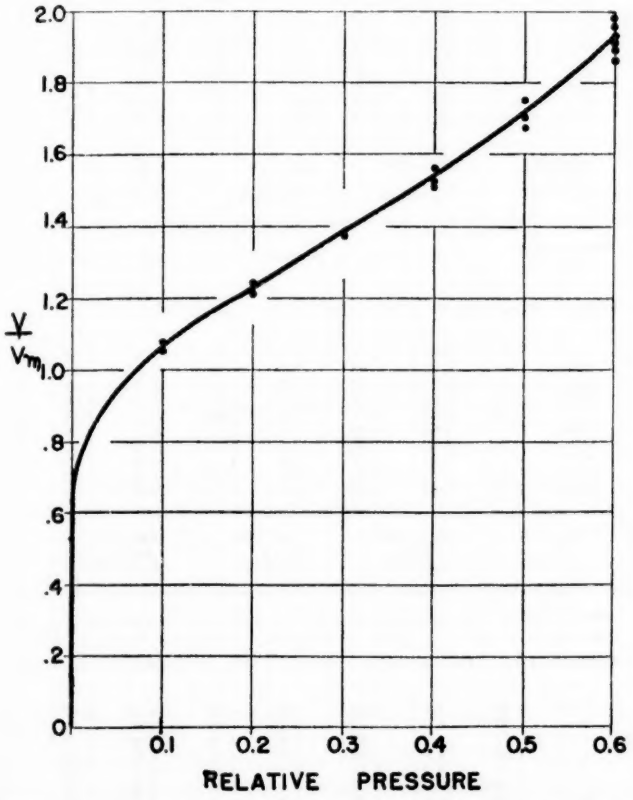


FIGURE 14.—*Adsorption isotherms of nitrogen on eight different bone chars at 77°K reduced to unit surface in a plot of $V/v_m$ against $p/p_0$*

For the data see table 2.

and then retained as a standard for laboratory filtration tests. Service char 3 is an example of a bone black in the latter stages of its effectiveness; spent char 15 had been discarded by the Revere Sugar Refinery; service char 14 was obtained from the Savannah Sugar Refinery; service char 8 is a good decolorizer, although the carbon had been reduced in revivification furnaces to 2.7 percent, leaving the material of a gray appearance. An experiment is planned in which a sample of bone char will be subjected to repeated decolorization and revivification cycles and the adsorption of nitrogen per unit surface determined at various stages. Such data will offer a better test for the constancy of the adsorption reduced to unit surface.

474862—42——3

TABLE 3.—*Value of $V/v_m$ for the adsorption of nitrogen on bone chars at 90° K*

[Values given under $V$ are in milliliters at STP]

| $x$ | New char 2 | | New char 2 | | New char 2 | | New char 2 | | Service char 9 | |
|---|---|---|---|---|---|---|---|---|---|---|
| | $V$(obs.) | $V/v_m$ | $V$(obs.) | $V/v_m$ | $V$(obs.) | $V/v_m$ | $V$(obs.) | $V/v_m$ | $V$(obs.) | $V/v_m$ |
| 0.03 | 22.7 | 0.88 | 22.2 | 0.87 | 22.8 | 0.87 | 22.1 | 0.87 | 15.2 | 0.85 |
| 0.06 | 25.3 | .98 | 24.9 | .98 | 25.7 | .98 | 24.0 | .94 | 17.2 | .96 |
| 0.08 | 26.3 | 1.02 | 26.1 | 1.03 | 26.7 | 1.02 | 25.0 | .98 | 18.0 | 1.01 |
| 0.12 | 28.3 | 1.09 | 28.0 | 1.10 | 28.7 | 1.10 | 27.0 | 1.06 | 19.4 | 1.09 |
| 0.15 | 29.5 | 1.14 | 29.2 | 1.15 | 29.9 | 1.14 | 28.5 | 1.12 | 20.4 | 1.14 |
| 0.18 | 30.7 | 1.19 | 30.4 | 1.19 | 31.1 | 1.19 | 30.0 | 1.18 | 21.2 | 1.18 |
| 0.20 | 31.5 | 1.22 | 31.1 | 1.23 | 31.9 | 1.22 | 30.7 | 1.21 | 21.8 | 1.21 |
| 0.24 | 33.1 | 1.28 | 32.6 | 1.28 | 33.4 | 1.28 | 32.3 | 1.27 | 22.8 | 1.27 |
| 0.27 | 34.2 | 1.33 | 33.7 | 1.33 | 34.5 | 1.32 | 33.5 | 1.32 | 23.6 | 1.32 |
| 0.30 | 35.3 | 1.37 | 34.8 | 1.37 | 35.6 | 1.37 | 34.6 | 1.36 | 24.4 | 1.36 |
| | Exp. 12–c $n=4$ $v_m=25.78$ | | Exp. 19–c $n=4$ $v_m=25.38$ | | Exp. 16–c $n=4$ $v_m=26.07$ | | Exp. 1 $n=4$ $v_m=25.49$ | | Exp. 17–a $n=4$ $v_m=17.97$ | |

| $x$ | Service char 8 (gray) | | Service char 3 | | Service char 3 | | New char 16 | | New char $C$ | |
|---|---|---|---|---|---|---|---|---|---|---|
| | $V$(obs.) | $V/v_m$ | $V$(obs.) | $V/v_m$ | $V$(obs.) | $V/v_m$ | $V$(obs.) | $V/v_m$ | $V$(obs.) | $V/v_m$ |
| 0.03 | 11.2 | 0.86 | 6.03 | 0.84 | 7.0 | 0.84 | 19.0 | 0.88 | 19.6 | 0.87 |
| 0.06 | 12.5 | .96 | 6.80 | .95 | 7.7 | .92 | 21.1 | .97 | 22.0 | .97 |
| 0.08 | 13.2 | 1.01 | 7.25 | 1.01 | 8.2 | .98 | 22.0 | 1.02 | 23.0 | 1.02 |
| 0.12 | 14.2 | 1.09 | 8.00 | 1.11 | 8.8 | 1.06 | 23.5 | 1.08 | 24.6 | 1.09 |
| 0.15 | 14.8 | 1.14 | 8.38 | 1.17 | 9.0 | 1.08 | 24.7 | 1.14 | 25.7 | 1.13 |
| 0.18 | 15.5 | 1.19 | 8.65 | 1.20 | 9.7 | 1.17 | 25.8 | 1.19 | 26.8 | 1.18 |
| 0.20 | 15.9 | 1.22 | 8.82 | 1.23 | 10.0 | 1.20 | 26.4 | 1.22 | 27.6 | 1.22 |
| 0.24 | 16.7 | 1.28 | 9.20 | 1.28 | 10.4 | 1.24 | 27.9 | 1.29 | 29.0 | 1.28 |
| 0.27 | 17.2 | 1.32 | 9.45 | 1.31 | 10.7 | 1.28 | 28.9 | 1.33 | 30.2 | 1.33 |
| 0.30 | 17.8 | 1.37 | 9.68 | 1.35 | 11.0 | 1.31 | 30.0 | 1.39 | 31.3 | 1.38 |
| | Exp. 17–a $n=4$ $v_m=13.06$ | | Exp. 16–e $n=4$ $v_m=7.19$ | | Exp. 19–c $n=4$ $v_m=8.37$ | | Exp. 20–j $n=5$ $v_m=21.65$ | | Exp. 21–b $n=5$ $v_m=22.64$ | |

| $x$ | Service char 14 | | Service char 14 | | Service char 12 | | Service char 3 | | Spent char 15 | |
|---|---|---|---|---|---|---|---|---|---|---|
| | $V$(obs.) | $V/v_m$ | $V$(obs.) | $V/v_m$ | $V$(obs.) | $V/v_m$ | $V$(obs.) | $V/v_m$ | $V$(obs.) | $V/v_m$ |
| 0.03 | 7.0 | 0.83 | 7.4 | 0.83 | 6.6 | 0.90 | 6.8 | 0.87 | 3.2 | 0.84 |
| 0.06 | 7.8 | .92 | 8.2 | .92 | 7.2 | .99 | 7.6 | .97 | 3.5 | .93 |
| 0.08 | 8.2 | .97 | 8.7 | .98 | 7.5 | 1.04 | 8.0 | 1.02 | 3.7 | .99 |
| 0.12 | 8.9 | 1.05 | 9.4 | 1.06 | 8.0 | 1.11 | 8.6 | 1.10 | 4.0 | 1.07 |
| 0.15 | 9.4 | 1.11 | 9.9 | 1.11 | 8.3 | 1.15 | 9.0 | 1.15 | 4.2 | 1.12 |
| 0.18 | 9.8 | 1.16 | 10.3 | 1.17 | 8.6 | 1.19 | 9.4 | 1.20 | 4.4 | 1.17 |
| 0.20 | 10.1 | 1.20 | 10.6 | 1.20 | 8.8 | 1.21 | 9.6 | 1.23 | 4.5 | 1.20 |
| 0.24 | 10.7 | 1.26 | 11.2 | 1.27 | 9.1 | 1.25 | 10.2 | 1.30 | 4.8 | 1.26 |
| 0.27 | 11.0 | 1.30 | 11.7 | 1.32 | 9.5 | 1.30 | 10.6 | 1.35 | 5.0 | 1.31 |
| 0.30 | 11.4 | 1.35 | 12.1 | 1.37 | 9.7 | 1.34 | 11.0 | 1.40 | 5.1 | 1.36 |
| | Exp. 8 $n=5$ $v_m=8.51$ | | Exp. 10 $n=5$ $v_m=8.89$ | | Exp. 1 $n=4$ $v_m=7.28$ | | Exp. 12–e $n=4$ $v_m=7.85$ | | Exp. 10 $n=4$ $v_m=3.82$ | |

| $x$ | Spread of $V/v_m$ for $n=4$ | | | Spread of $V/v_m$ for $n=5$ | | |
|---|---|---|---|---|---|---|
| | Min. | Max. | Deviation | Min. | Max. | Deviation |
| | | | % | | | % |
| 0.03 | 0.84 | 0.90 | 6 | 0.83 | 0.88 | 6 |
| 0.06 | .92 | .99 | 7 | .92 | .97 | 6 |
| 0.08 | .98 | 1.03 | 5 | .97 | 1.02 | 5 |
| 0.12 | 1.06 | 1.11 | 5 | 1.05 | 1.09 | 4 |
| 0.15 | 1.08 | 1.17 | 8 | 1.11 | 1.14 | 3 |
| 0.18 | 1.17 | 1.20 | 3 | 1.16 | 1.19 | 2 |
| 0.20 | 1.20 | 1.23 | 3 | 1.20 | 1.22 | 2 |
| 0.24 | 1.24 | 1.30 | 5 | 1.26 | 1.29 | 3 |
| 0.27 | 1.28 | 1.35 | 5 | 1.30 | 1.33 | 3 |
| 0.30 | 1.31 | 1.40 | 5 | 1.35 | 1.39 | 3 |

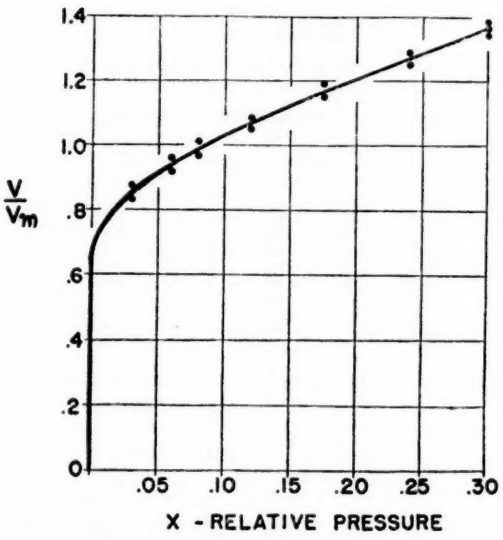


FIGURE 15.—*Adsorption isotherms of nitrogen on eight different bone chars at 90° K reduced to unit surface in a plot of $V/v_m$ against $p/p_0$.*

For the data see table 3.

A possible interpretation of these results is to be found in attributing approximately the same pore-size distribution to all the bone char samples investigated. Moreover in these adsorption measurements the fraction of surface covered varies between $0.8v_m$ to $2v_m$. Consequently, the determinations are being made on the most uniform portion of the surface, since the active or other heterogeneous regions have already been covered in the early stages. In this manner a pure surface effect is measured which is independent of chemisorptive influences.

The results for the samples other than bone black show analogous behavior but with significant differences for the value of $n$. Tables 4 and 5 are obtained from the data on such samples. The isotherms for the chars with the value of $n=2$ fall into a group about a single reduced isotherm; similarly, the two carbons with $n=1.5$ constitute another group. If one considers the data for all the adsorbents, including the coconut-shell charcoals, five curves are characterized by $n=1$, 1.5, 2, 4, or 5, and these suffice to plot the nitrogen adsorption per unit surface. These reduced isotherms are illustrated in figures 16 and 17. The conclusion may be drawn that the value of $n$ is a quantitative index, of limited accuracy, of the maximum average diameter of those pores effective in adsorption at relative pressures less than 0.6.

TABLE 4.—*Values of $V/v_m$ for the adsorption of nitrogen on carbons other than bone char at 77°K*

[Values given under $V$ are in milliliters at STP]

| $x$ | Vegetable carbon 5 | | Activated carbon 6 | | Activated carbon 19 | | Activated carbon 20 | |
|---|---|---|---|---|---|---|---|---|
| | $V$ (obs.) | $V/v_m$ | $V$ (obs.) | $V/v_m$ | $V$ (obs.) | $V/v_m$ | $V$ (obs.) | $V/v_m$ |
| 0.1 | 206 | 0.98 | 130 | 1.01 | 337 | 1.10 | 115 | 0.99 |
| 0.2 | 233 | 1.11 | 143 | 1.11 | 355 | 1.16 | 130 | 1.12 |
| 0.3 | 251 | 1.19 | 152 | 1.18 | 375 | 1.22 | 138 | 1.19 |
| 0.4 | 268 | 1.27 | 164 | 1.27 | 392 | 1.28 | 147 | 1.27 |
| 0.5 | 283 | 1.34 | 173 | 1.34 | 408 | 1.34 | 156 | 1.34 |
| 0.6 | 298 | 1.41 | 183 | 1.42 | 425 | 1.39 | 165 | 1.42 |
| 0.7 | 310 | 1.47 | 192 | 1.49 | 443 | 1.45 | 176 | 1.51 |
| | Exp. 15–a $n=2$ $v_m=211$ | | Exp. 15–a $n=2$ $v_m=129$ | | Exp. 20–a $n=2$ $v_m=306$ | | Exp. 20–a $n=2$ $v_m=116$ | |

| $x$ | Vegetable carbon 4 | | Activated carbon 18 | |
|---|---|---|---|---|
| | $V$ (obs.) | $V/v_m$ | $V$ (obs.) | $V/v_m$ |
| 0.1 | 220 | 1.03 | 336 | 1.02 |
| 0.2 | 230 | 1.08 | 356 | 1.08 |
| 0.3 | 239 | 1.12 | 368 | 1.12 |
| 0.4 | 246 | 1.15 | 377 | 1.14 |
| 0.5 | 252 | 1.18 | 384 | 1.16 |
| 0.6 | 260 | 1.22 | 393 | 1.19 |
| 0.7 | 270 | 1.26 | 403 | 1.22 |
| | Exp. 15–a $n=1.5$ $v_m=214$ | | Exp. 23 $n=1.5$ $v_m=330$ | |

| $x$ | Spread of $V/v_m$ for $n=1.5$ | | | Spread of $V/v_m$ for $n=2$ | | |
|---|---|---|---|---|---|---|
| | Min. | Max. | Deviation | Min. | Max. | Deviation |
| | | | *Percent* | | | *Percent* |
| 0.1 | 1.02 | 1.03 | 1 | 0.98 | 1.10 | 10 |
| 0.2 | 1.08 | 1.08 | 0 | 1.11 | 1.16 | 5 |
| 0.3 | 1.12 | 1.12 | 0 | 1.18 | 1.22 | 3 |
| 0.4 | 1.14 | 1.15 | 1 | 1.27 | 1.28 | 1 |
| 0.5 | 1.16 | 1.18 | 2 | 1.34 | 1.34 | 0 |
| 0.6 | 1.19 | 1.22 | 3 | 1.39 | 1.42 | 2 |
| 0.7 | 1.22 | 1.26 | 3 | 1.44 | 1.51 | 5 |

TABLE 5.—*Values of $V/v_m$ for the adsorption of nitrogen on carbons other than bone char at 90° K*

[Values given under $V$ are in milliliters at STP]

| $x$ | Vegetable carbon 5 | | Activated carbon 6 | | Activated carbon 19 | | Activated carbon 20 | |
|---|---|---|---|---|---|---|---|---|
| | $V$(obs.) | $V/v_m$ | $V$(obs.) | $V/v_m$ | $V$(obs.) | $V/v_m$ | $V$(obs.) | $V/v_m$ |
| 0.05 | 177 | 0.96 | 117 | 0.98 | 262 | 0.94 | 100 | 0.97 |
| 0.10 | 193 | 1.05 | 126 | 1.06 | 289 | 1.04 | 108 | 1.04 |
| 0.15 | 203 | 1.09 | 132 | 1.11 | 305 | 1.09 | 113 | 1.09 |
| 0.20 | 211 | 1.14 | 137 | 1.15 | 318 | 1.14 | 118 | 1.14 |
| 0.25 | 218 | 1.18 | 142 | 1.20 | 328 | 1.18 | 122 | 1.18 |
| 0.30 | 225 | 1.22 | 147 | 1.24 | 338 | 1.21 | 125 | 1.21 |
| | Exp. 18–d $n=2$ $v_m=184.7$ | | Exp. 18–d $n=2$ $v_m=118.7$ | | Exp. 20–j $n=2$ $v_m=279.0$ | | Exp. 20–j $n=2$ $v_m=103.3$ | |

| $x$ | Activated carbon 18 | | Vegetable carbon 4 | | Vegetable carbon 4 | |
|---|---|---|---|---|---|---|
| | $V$(obs.) | $V/v_m$ | $V$(obs.) | $V/v_m$ | $V$(obs.) | $V/v_m$ |
| 0.05 | 282 | 0.94 | 196 | 0.97 | 194 | 0.97 |
| 0.10 | 304 | 1.01 | 208 | 1.03 | 206 | 1.03 |
| 0.15 | 317 | 1.06 | 216 | 1.07 | 212 | 1.06 |
| 0.20 | 325 | 1.08 | 219 | 1.09 | 219 | 1.09 |
| 0.25 | 332 | 1.11 | 225 | 1.12 | 222 | 1.11 |
| 0.30 | 340 | 1.13 | 229 | 1.14 | 225 | 1.13 |
| | Exp. 11 $n=1.5$ $v_m=300$ | | Exp. 18–d $n=1.5$ $v_m=201.7$ | | Exp. 15–i $n=1.5$ $v_m=200.1$ | |

| $x$ | Spread of $V/v_m$ for $n=1.5$ | | | Spread of $V/v_m$ for $n=2$ | | |
|---|---|---|---|---|---|---|
| | Min. | Max. | Deviation | Min. | Max. | Deviation |
| | | | % | | | % |
| 0.05 | 0.94 | 0.97 | 4 | 0.94 | 0.98 | 5 |
| 0.10 | 1.01 | 1.03 | 2 | 1.04 | 1.06 | 2 |
| 0.15 | 1.06 | 1.07 | 1 | 1.09 | 1.11 | 2 |
| 0.20 | 1.08 | 1.09 | 1 | 1.14 | 1.15 | 1 |
| 0.25 | 1.11 | 1.12 | 1 | 1.18 | 1.20 | 2 |
| 0.30 | 1.13 | 1.14 | 1 | 1.21 | 1.24 | 2 |

TABLE 6.—*Value of $V/v_m$ for the adsorption of nitrogen on coconut charcoal*

| $x$ | Charcoal 1 | | Charcoal 17 | |
|---|---|---|---|---|
| | $V$ | $V/v_m$ | $V$ | $V/v_m$ |
| | at 77°K | | | |
| | *ml at STP* | | *ml at STP* | |
| 0.1 | 306 | 0.71 | 276 | 0.8 |
| 0.2 | 359 | .84 | 294 | .9 |
| 0.3 | 380 | .88 | 305 | .9 |
| 0.4 | 391 | .91 | 309 | .9 |
| 0.5 | 397 | .92 | 312 | .9 |
| 0.6 | 403 | .94 | 314 | .9 |
| 0.7 | 407 | .95 | 316 | .9 |
| 0.8 | 409 | .95 | 318 | .9 |
| | Exp. 14-a<br>$n=1$<br>$v_m=430$ | | Exp. 24-c<br>$n=1$<br>$v_m=323$ | |
| | at 90°K | | | |
| 0.05 | 289 | 0.79 | 245 | 0.8 |
| 0.10 | 322 | .88 | 266 | .9 |
| 0.15 | 377 | .92 | 275 | .9 |
| 0.20 | 345 | .94 | 279 | .9 |
| 0.25 | 350 | .95 | 282 | .9 |
| | Exp. 16-a<br>$n=1$<br>$v_m=367$ | | Exp. 24-b<br>$n=1$<br>$v_m=293$ | |

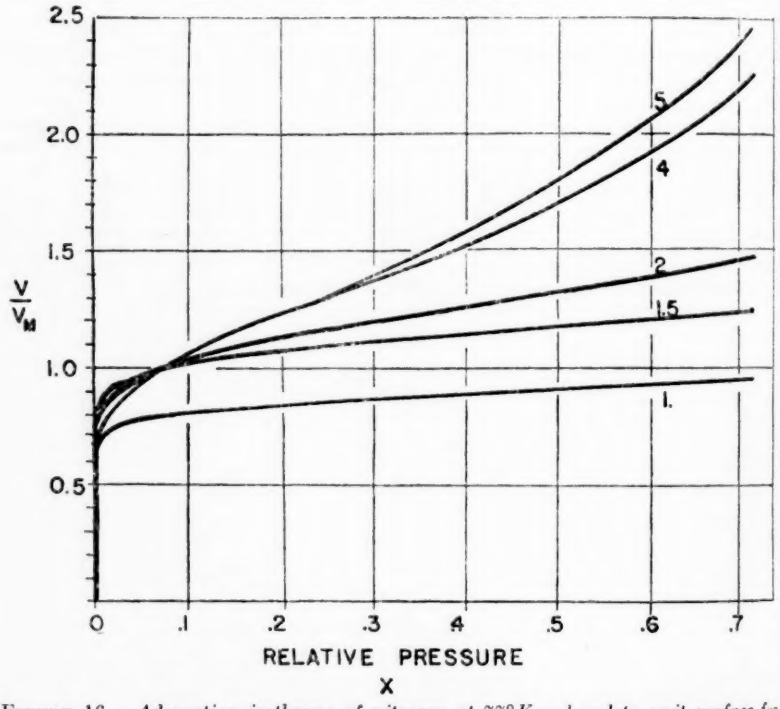


FIGURE 16.—*Adsorption isotherms of nitrogen at 77°K reduced to unit surface for the five classes of adsorbents characterized by $n=1$, 1.5, 2, 4, and 5.*

For the data, see tables 2, 4, and 6.

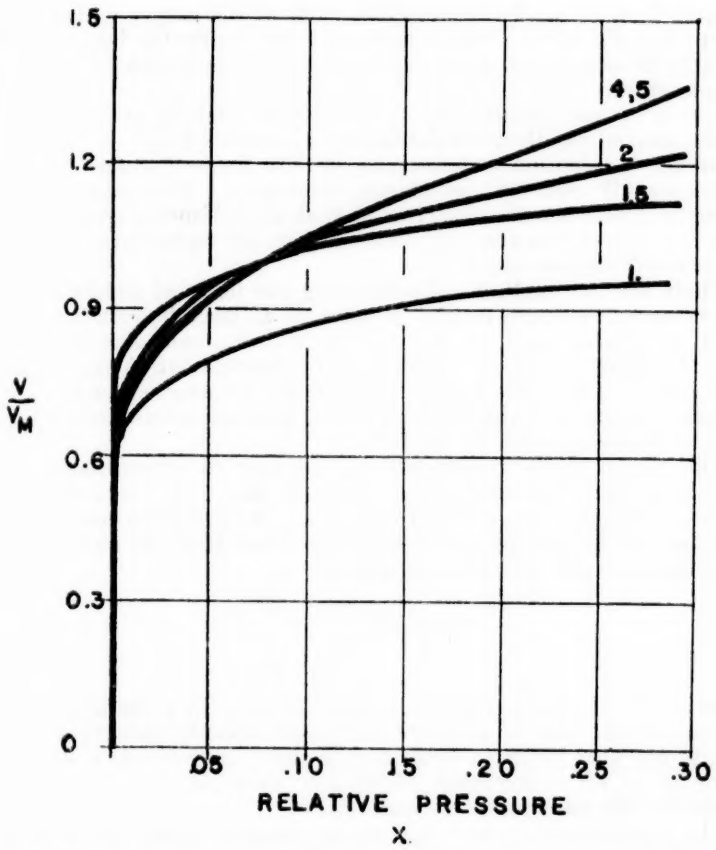


FIGURE 17.—*Adsorption isotherms of nitrogen at 90° K reduced to unit surface for the five classes of adsorbents characterized by n=1, 1.5, 2, 4, and 5.*

For the data see tables 3, 5, and 6.

The question may arise as to whether the method of determining $v_m$ would necessarily lead to identical values of $V/v_m$ at a given value of $x$ for all the bone chars. However, from eq 1 it is seen that $V/v_m$ at a given value of $x$ is a function of $n$, and thus for a given value of $n$, $V/v_m$ depends only on $c$. But from the nature of van der Waals' forces of adsorption, $c$ is substantially constant for the same type of materials in this pressure range. Therefore the equivalence of the adsorption per unit surface is verification of a similar distribution of pore sizes in all those samples in which $n$ is the same.

## V. HEATS OF ADSORPTION

As the process of adsorption progresses from the earliest stages to saturation, the heat of adsorption may change somewhat as follows: (1) Designating $E_L$ as the heat of liquefaction and $E_1$ as the average heat of adsorption on the first layer, the heat of adsorption may be

greater than $E_1$ on the most active parts of the empty surface; (2) it is equal to $E_1$, which corresponds to adsorption on the less active and roughly homogeneous part of the surface; (3) following this, the heat of adsorption approaches $E_L$ as the polymolecular layers form; (4) the heat of adsorption may again become slightly greater than $E_L$ as the heat of capillary condensation is liberated [12].

In the adsorption experiments of this investigation the above processes (2) and (3) are chiefly concerned. The region of good agreement between the observed and calculated isotherms is for values of $V/v_m$ from 0.8 to about 2, which is just the region where processes (2) and (3) may occur.

There are two methods of estimating the heats of adsorption from the nitrogen isotherm data. A value of $E_1$ may be calculated from eq 1 by noting that in the theory of multimolecular adsorption, $E_1-E_L=2.303\,RT\log c$. The results of this calculation are assembled in table 7. The value for the molal heat of vaporization at 77.3° K is 1,332.9 calories, and at 90.0° K, 1,510 calories, as obtained from the data of Giauque and Clayton [13].

The second method of evaluating the heat of adsorption is to use the Clapeyron-Clausius equation with the data from the isotherms at the two temperatures, 90° and 77.3° K. The pressures corresponding to equal amounts of adsorbate are determined from the isotherms and substituted in the following equation:

$$q_V=2.303R\frac{\log p_1-\log p_2}{\frac{1}{T_2}-\frac{1}{T_1}}.$$

Here $q_V$ is the differential heat of adsorption at a definite value of $V$, and $p$ and $T$ are the pressure and the absolute temperature. These results are also given in table 6 and show, in general, a decreasing value of $q_V$ with increasing adsorption, as required by the assumed model for the adsorptive mechanism.

The agreement between the two methods is rather satisfactory in view of the uncertainties involved. The same amount of adsorbate at two different temperatures may not be in strictly comparable conditions. Something comparable to this situation must exist for the adsorbents of high surface having a value of $n=1$, 1.5, and 2, since the surface determined at the lower temperature is appreciably greater. It is to be noted in table 6 that the value for $q_V$ decreases toward $E_L$ as the volume adsorbed increases.

Table 7 contains the calculated $E_1$ values from each isotherm at the two temperatures. The difference between the two, $\Delta E_1$, is on the average greater than the difference between the heats of vaporization, namely $E_L(90°)-E_L(77.3°)=1,510-1,335=175$ calories.

TABLE 7.—*Comparison of $E_1$ with the calculated differential heats of adsorption*

| Sample | $T$ | $E_1-E_L$ | $E_1$ | $\Delta E_1$ | Differential heats of adsorption (in calories) |
|---|---|---|---|---|---|
| | ° K | *Calories* | *Calories* | *Calories* | |
| 2 | 76.4 | 890 | 2,230 | 240 | $q(V=25)=2,145$ |
| 2 | 89.7 | 945 | 2,470 | | $q(V=30)=1,760$ |
| | | | | | $q(V=35)=1,620$ |
| C | 77.3 | 850 | 2,180 | 240 | $q(V=25)=1,930$ |
| C | 90.1 | 910 | 2,420 | | $q(V=30)=1,660$ |

TABLE 7.—*Comparison of $E_1$ with the calculated differential heats of adsorption*—Continued

| Sample | $T$ | $E_1-E_L$ | $E_1$ | $\Delta E_1$ | Differential heats of adsorption (in calories) |
|---|---|---|---|---|---|
| | ° *K* | *Calories* | *Calories* | *Calories* | |
| *B* | 77.3 | 860 | 2,190 | 200 | $q(V=25)=1,860$ |
| *B* | 90.1 | 880 | 2,390 | | $q(V=30)=1,560$ |
| 16 | 77.2 | 930 | 2,260 | 160 | $q(V=25)=2,230$ |
| 16 | 89.3 | 905 | 2,415 | | $q(V=30)=1,750$ |
| 16 | 90.4 | 905 | 2,415 | | |
| 3 | 76.4 | 930 | 2,260 | 110 | $q(V=9)=2,440$ |
| 3 | 89.7 | 860 | 2,370 | | |
| 8 | 77.0 | 900 | 2,240 | 120 | $q(V=12)=2,230$ |
| 8 | 89.8 | 840 | 2,350 | | $q(V=15)=1,850$ |
| | | | | | $q(V=18)=1,590$ |
| 9 | 77.0 | 760 | 2,100 | 290 | $q(V=18)=2,050$ |
| 9 | 89.8 | 880 | 2,390 | | $q(V=21)=1,800$ |
| 14 | 77.2 | 780 | 2,110 | 220 | $q(V=9)=2,450$ |
| 14 | 89.7 | 820 | 2,330 | | $q(V=11)=1,650$ |
| 14 | 89.5 | 810 | 2,320 | | |
| 14 | 89.4 | 830 | 2,340 | | |
| 12 | 77.8 | 810 | 2,140 | 340 | $q(V=8)=2,350$ |
| 12 | 89.5 | 980 | 2,480 | | $q(V=9)=2,300$ |
| 15 | 77.8 | 785 | 2,120 | 230 | $q(V=4)=2,320$ |
| 15 | 89.4 | 845 | 2,350 | | $q(V=5)=1,860$ |
| 4 | 76.6 | 775 | 2,110 | 410 | $q(V=215)=2,200$ |
| 4 | 89.6 | 1,000 | 2,510 | | $q(V=225)=2,020$ |
| 4 | 89.9 | 1,020 | 2,530 | | |
| 5 | 76.6 | 700 | 2,040 | 410 | $q(V=190)=2,040$ |
| 5 | 89.6 | 930 | 2,440 | | $q(V=200)=2,010$ |
| 5 | 89.9 | 950 | 2,460 | | |
| 6 | 76.6 | 710 | 2,050 | 430 | $q(V=120)=2,130$ |
| 6 | 89.6 | 890 | 2,400 | | |
| 6 | 89.9 | 1,040 | 2,560 | | |
| 19 | 77.3 | 805 | 2,140 | 280 | $q(V=330)=2,630$ |
| 19 | 90.4 | 910 | 2,420 | | $q(V=340)=2,480$ |
| 20 | 77.3 | 865 | 2,200 | 270 | $q(V=110)=2,440$ |
| 20 | 90.4 | 960 | 2,470 | | $q(V=120)=2,200$ |
| 18 | 77.6 | 820 | 2,150 | 290 | $q(V=340)=2,420$ |
| 18 | 89.3 | 925 | 2,440 | | |
| 1 | 76.4 | 490 | 1,830 | 440 | $q(V=350)=2,000$ |
| 1 | 89.7 | 760 | 2,270 | | |
| 17 | 77.6 | 650 | 1,990 | 350 | $q(V=290)=2,380$ |
| 17 | 90.0 | 830 | 2,340 | | |
| Carbon black | 77.6 | 780 | 2,110 | 230 | $q(V=25)=1,890$ |
| Do | 90.0 | 830 | 2,340 | | $q(V=30)=1,720$ |

## VI. DEPENDENCE OF THE ADSORPTION ON CAPILLARITY

It has been shown that the nitrogen isotherms obtained in these experiments may be interpreted by means of the multimolecular adsorption theory of Brunauer, Emmett, and Teller for values of $x$ from 0.1 to 0.5 for bone-char samples as well as for vegetable carbons. In this theory the concept of capillarity enters through the restriction of multimolecular adsorption caused by the proximity of plane parallel walls between which the adsorption takes place. The region of adsorption between $x=0.5$ and saturation might most probably be

interpreted, at least from a qualitative point of view, in terms of a change in pore-size distribution. As the adsorption progresses and the multimolecular layers form in appreciable amounts, the smaller capillaries are filled. The remaining available distribution is thus dominated by the larger unfilled capillaries.

Since the theory of multimolecular adsorption, as expressed in eq 1, is not accurate enough to account for the adsorption at higher pressures, and the more elaborate equations of Brunauer, Deming, Deming, and Teller [12] are too difficult to handle mathematically, it may be of interest to examine the data in terms of the capillary condensation theory. From this theory it follows that condensation must occur in cylindrical capillaries according to the Kelvin equation:

$$\ln p/p_0 = \frac{-2\gamma v}{rRT}. \tag{4}$$

Here $\gamma$ is the surface tension; $v$ is the molar volume of the liquid; $R$ is the gas constant, equal to $8.314\times10^7$ ergs per degree; $T$ is the absolute temperature; and $r$ is the radius of the concave meniscus. This theory impiles that all capillaries of the same uniform cross section will be either empty or else be completely filled. Experimen-

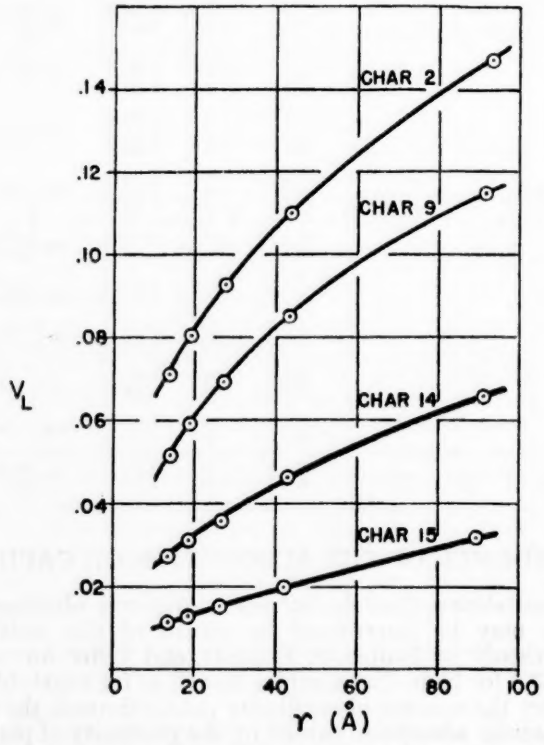


FIGURE 18.—*Adsorption at 77° K on bone chars in a plot of the volume of liquid nitrogen adsorbed, $V_L$, per gram of adsorbent against the corresponding radius of a cylindrical capillary as determined from the Kelvin equation.*

The five points in circles correspond to $x=0.5, 0.6, 0.7, 0.8, 0.9$, respectively.

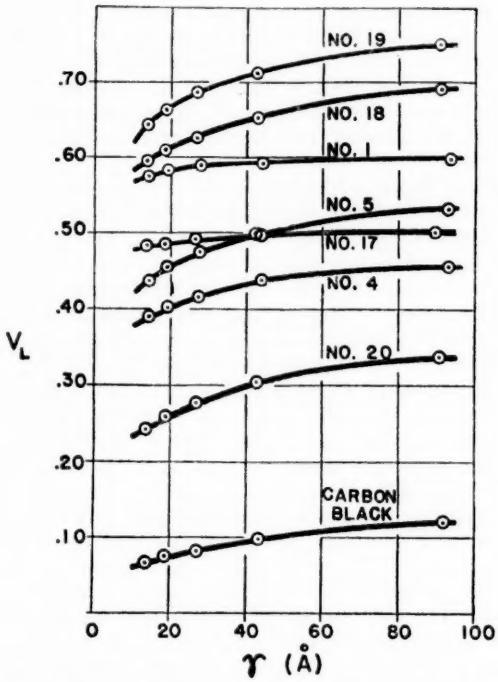


FIGURE 19.—*Adsorption at 77° K on adsorbent carbons other than bone char in a plot of the volume of liquid nitrogen, $V_L$, per gram of adsorbent against the corresponding radius of a cylindrical capillary as determined from the Kelvin equation.*

The five points in circles correspond to $x=0.5$, 0.6, 0.7, 0.8, and 0.9, respectively.

tally the sharp rise in adsorption demanded by the theory has never been found. This has been explained by assuming a continuously varying distribution of the cross sections of the capillaries.

From eq 4 a value of $2r$ equal to 30 A is obtained for nitrogen at 77° K to correspond to the value of $p/p_0$ equal to 0.5. Since the diameter of the nitrogen molecule considered as a sphere in the liquid state is 4.3 A, a diameter of 30 A is of plausible order of magnitude for capillary condensation phenomena. In figures 18 and 19 the volume of liquid adsorbed, $V_L$, is plotted against $r$ for a number of materials included in this paper. To express the adsorption in milliliters of liquid nitrogen, the density of nitrogen gas at 0° and 760 mm was taken to be 1.2506 g per liter [13]. Equation 4 was used to calculate $r$ from the data of the experiment along with the required constants in the International Critical Tables.

It can be seen from the graphs of $V_L$ against $r$ in figure 19 that the slopes of the curves for carbons other than bone char seem to be approaching zero as the adsorption increases. According to the theory of capillary condensation, this would mean that there are only a relatively small number of pores with large radii. The major part of the adsorption on the carbons other than bone chars appears to occur in capillaries of less than 20 A radius. A distribution curve for the capillaries would, therefore, have a relatively narrow breadth and

a maximum somewhere in the region of very narrow capillaries. However, the adsorption for the bone chars shows a much steeper rise, as may be seen from figure 18, where about half of the adsorption takes place in capillaries greater than 20 A. Consequently a distribution curve for a bone char would have a greater breadth to indicate the presence of capillaries of larger cross section available for adsorption.

No matter what the mechanism of the adsorption at low values of $p/p_0$, it is reasonable to think that the narrow interstices in the structure of the adsorbent promote adsorption. From purely thermodynamic considerations this may occur whenever the adsorbate is confined to regions small enough to change the escaping tendency from the value for the liquid state. Condensation must occur, therefore, at the higher pressures in the small interstices between broken crystal aggregates. However, it cannot be quantitatively stated at present how closely it is necessary to approach saturation pressure in order to obtain an appreciable contribution to adsorption from this source.

The success of the multimolecular theory of Brunauer, Emmett, and Teller in the pressure range between $x=0.05$ and 0.5 leads to a consideration of the difficulties with the theory in the high-pressure range. The derivation of the equations is based on a model involving condensation on and evaporation from the various layers in multimolecular adsorption. The value of $V$ corresponding to $v_m$ does not mean that at this point the surface is completely covered with a unimolecular layer. On the contrary, appreciable amounts of layers of two, three, and even four molecules in thickness may be present. In this mechanism a statistical equilibrium between layers of adsorbed molecules is postulated. A complete statistical theory involving the evaporation and condensation of individual molecules would take into account the interaction of neighbors within the layer and thus approach more closely to the actual situation at the higher relative pressures.

One of the main achievements of the theory of multimolecular adsorption as embodied in the papers of Brunauer, Emmett, and Teller [6] and Brunauer, Deming, Deming, and Teller [12] is that it gives a complete picture of van der Waals' adsorption, and accounts for the variety of different-shaped isotherms that can be found in the literature. Although there are difficulties with a quantitative application of the theory close to saturation pressures, it accounts quantitatively for all of the isotherms given in this paper up to about $p/p_0=0.6$. For the purpose of this investigation the most important feature is that it enables one to calculate relative values for the specific surfaces of adsorbents with a fair degree of accuracy.

---

We express our appreciation to Stephen Brunauer, of the Bureau of Plant Industry, United States Department of Agriculture, and to P. H. Emmett, of the John Hopkins University, for valuable discussions on the principles of adsorption involved in this paper. We also express our appreciation to Eloise A. Swick for her assistance in the calculations.

## VII. REFERENCES

[1] F. Paneth, Z. Elektrochem. **28,** 113 (1922).
[2] P. C. Carman, J. Soc. Chem. Ind. **58,** 1 (1939).
[3] S. S. Kistler, J. Phys. Chem. **46,** 19 (1942).
[4] P. H. Emmett and S. Brunauer, J. Am. Chem. Soc. **59,** 1553 (1937).
[5] S. Brunauer and P. H. Emmett, J. Am. Chem. Soc. **59,** 2682 (1937).
[6] S. Brunauer, P. H. Emmett, and E. Teller, J. Am. Chem. Soc. **60,** 309 (1938).
[7] P. H. Emmett and T. De Witt, Ind. Eng. Chem., Anal. Ed. **13,** 28 (1941).
[8] W. R. Smith, F. S. Thornhill, and R. I. Bray, Ind. Eng. Chem. **33,** 1303 (1941).
[9] C. T. Lane and W. W. Watson, Rev. Sci. Instr. **11,** 272 (1940).
[10] V. R. Deitz and L. F. Gleysteen, J. Research NBS **28,** 795–805 (1942) RP 1479.
[11] I. Langmuir, J. Am. Chem. Soc. **37,** 1139 (1915).
[12] S. Brunauer, L. S. Deming, W. E. Deming, and E. Teller, J. Am. Chem. Soc. **62,** 1723 (1940).
[13] W. F. Giauque and J. O. Clayton, J. Am. Chem. Soc. **55,** 4881 (1933).
[14] P. H. Emmett, Am. Soc. Testing Materials, Symposium on New Methods for Particle Size Determination in Subsieve Range, **41,** 95–106 (1941).

WASHINGTON, June 26, 1942.

U. S. DEPARTMENT OF COMMERCE NATIONAL BUREAU OF STANDARD

RESEARCH PAPER RP1497

*Part of Journal of Research of the National Bureau of Standards, Volume 29, September 1942*

# PREPARATION OF LOWER ALDONIC ACIDS BY OXIDATION OF SUGARS IN ALKALINE SOLUTION

By Horace S. Isbell

ABSTRACT

Directions are given for the preparation of *l*-erythronic, *d*-threonic, *d*-lyxonic, *l*-xylonic, and *d*-arabonic acids by means of oxidation with oxygen of certain sugars in alkaline solution. *d*-Arabonic acid was obtained in about 70-percent yield, in agreement with the results of prior investigators. Lower yields were obtained for other aldonic acids, and they do not differ greatly from those obtained by oxidation with air. Nevertheless, the simplicity of the method makes it suitable for the production of lower aldonic acids by persons requiring a supply of these scarce materials. *l*-Erythronic and *d*-threonic acids were separated in the form of brucine salts, the optical rotations of which were found to be represented by the following expressions: $[\alpha]_D^{20} = -28.4 - 0.85C + 0.025C^2$, in which $C$ is the grams of anhydrous brucine *l*-erythronate in 100 ml of aqueous solution; and $[\alpha]_D^{20} = -28.5 - 0.9C + 0.025C^2$, in which $C$ is the grams of anhydrous brucine *d*-threonate in 100 ml of aqueous solution.

CONTENTS

| | | Page |
|---|---|---|
| I. | Introduction | 227 |
| II. | Oxidation method | 228 |
| III. | Preparation of brucine *l*-erythronate from *l*-arabinose | 229 |
| IV. | Preparation of brucine *d*-threonate from *d*-xylose | 230 |
| V. | Conversion of brucine *l*-erythronate or *d*-threonate to the corresponding acid | 231 |
| VI. | Preparation of cadmium *l*-xylonate-cadmium bromide from *l*-sorbose | 231 |
| VII. | Preparation of *d*-lyxono-γ-lactone from *d*-galactose | 231 |
| VIII. | Preparation of calcium *d*-arabonate from *d*-glucose | 232 |
| IX. | References | 232 |

## I. INTRODUCTION

From a study of the oxidation of reducing sugars with air in alkaline solution, Nef and his collaborators [1] [1] found that under the influence of alkali a reducing sugar forms a 1,2-enediol which undergoes oxidation and yields formic acid in addition to an acid containing one less carbon than the parent sugar. The over-all reaction appears to be represented by the following equation:

$$CH_2OH(CHOH)_nCHOH.CHO + O_2 \rightarrow CH_2OH(CHOH)_nCOOH + HCOOH.$$

By using oxygen in place of air, Splengler and Pfannenstiel [2] developed a method for the preparation of potassium *d*-arabonate from dextrose in 60 to 75 percent of the theoretical yield.

[1] Figures in brackets indicate the literature references at the end of this paper.

Subsequently, by essentially the same procedure, Neuberg and Collatz [3] obtained *d*-arabonic-5-phosphoric acid as the barium salt from fructose-5-phosphoric acid in 89-percent yield, whereas Richtmyer, Hann, and Hudson [4] obtained *l*-galactonic acid as the potassium salt from perseulose in 45-percent yield and *d*-altronic acid as the calcium salt from sedoheptulose in approximately 20-percent yield.[2]

From these publications it was obvious that the oxidation of reducing sugars with oxygen in alkaline solution provides a convenient means for obtaining the lower acids. A supply of *l*-erythronic, *d*-threonic, *l*-xylonic, *d*-lyxonic, and *d*-arabonic acids was needed for other investigations, and hence the preparation of these acids was undertaken by the oxidation of *l*-arabinose, *d*-xylose, *l*-sorbose, *d*-galactose, and *d*-glucose, respectively. Previously, Nef and his collaborators had prepared *l*-erythronic, *d*-threonic, and *d*-lyxonic acids in yields of about 30 percent, by oxidation of *l*-arabinose, *d*-xylose, and *d*-galactose with air in alkaline solution, and it seemed probable that much higher yields might be obtained by the use of pure oxygen. Experiments with oxygen appeared to proceed smoothly, and titrations indicated the production of only slightly more acid than that corresponding to the reaction of eq 1. Nevertheless, it was not possible to separate the desired products in high yield. The simplicity of the process, however, makes it practical for the production of pentonic and tetronic acids from sugars which are not very difficult to obtain. The preparation of *l*-xylonic acid from *l*-sorbose is particularly noteworthy, because *l*-xylonic acid can be used as an intermediate in the preparation of ascorbic acid.

## II. OXIDATION METHOD

The following procedure was employed for the oxidation of the sugars and for the preparation of the solutions of the nonvolatile acids. In each case 0.05 mole of the sugar was added to 200 ml. of 0.85 *N* potassium hydroxide solution, previously cooled to 0° C, and saturated with oxygen. The solution, in a thick-walled flask, was mixed on a shaking machine with oxygen at a pressure of from 5 to 15 pounds per square inch until the absorption of oxygen ceased (about 24 hours), after which 5 *N* hydrochloric acid was added from a burette in amount equivalent to the potassium hydroxide originally used. The solution was evaporated under reduced pressure to a thin sirup, which was diluted with 50 ml of water and evaporated a second time to substantial dryness to remove all volatile acids. The residue in the flask was digested with 25 ml of hot isopropyl alcohol (99 percent), and cooled to room temperature. After sufficient time for crystallization to take place, the potassium chloride was separated by filtration, washed with hot absolute alcohol, and discarded.[3] One gram of decolorizing carbon was added to the alcoholic filtrate and the mixture was given a second filtration to obtain a clear alcoholic solution of the nonvolatile acids.

[2] A total of 5.1 g of $Ca(C_6H_{11}O_7)_2 \cdot 3.5H_2O$ was obtained from two crude sedoheptulose solutions estimated to contain 10.5 g of sedoheptulose each.

[3] In each case the potassium chloride residue was tested to make certain that organic material was not discarded; sometimes a second washing with hot alcohol was necessary.

## III. PREPARATION OF BRUCINE *l*-ERYTHRONATE FROM *l*-ARABINOSE

The alcoholic solution of nonvolatile acids obtained from the oxidation of 0.05 mole of *l*-arabinose was mixed with 23 g (0.05 mole) of brucine dissolved in 100 ml of hot 95 percent alcohol. The mixture was placed in a refrigerator and was allowed to stand, with occasional stirring, for 24 hours while crystallization took place. The resulting crystals were collected on a filter and washed with 95 percent alcohol. The air-dried product weighed 17.5 g and melted at 190° to 195° C. The mother liquor was evaporated to a sirup (about 15 ml) which after saturation with isopropyl alcohol gave 3.4 g of crystals with a melting point of approximately 115° C. The second mother liquor gave additional crystals weighing 2.7 g and melting at 205° C. The first crop of material (mp, 190° to 195° C) was heated to boiling with 15 ml of absolute alcohol, and the mixture was cooled and filtered. The crystals on the filter were washed with 10 ml of absolute alcohol, and the filtrate and washings were used to extract the second crop (mp, 115° C), with the result that the melting point was raised to 200° C. The crystalline fractions which remained at this point melted above 200° C and had a combined weight of 18.7 g. By recrystallization from hot ethyl alcohol (600 ml) and concentration of the mother liquors, a total of 13 g of substantially pure brucine *l*-erthyronate was obtained.[4] The yield of brucine *l*-erythronate, 43 percent, was only slightly higher than that obtained by Nef, Hedenberg, and Glattfeld [5] by oxidation of *l*-arabinose with air.

For analysis the material was recrystallized again from hot alcohol and dried at room temperature in air. The substance separates in slender truncated prisms which melt at 212° C and give the following analysis: Calculated for $C_4H_8O_5 \cdot C_{23}H_{26}O_4N_2$: · C, 61.12; H, 6.46. Found: C, 61.38; H, 6.30. The specific rotation in water at a concentration of 4 g per 100 ml of solution was found to be appreciably higher than the value −28.4 reported for brucine *l*-erythronate at the same concentration by Ruff [6] and by Neuberg and Hirschberg [7]. However, by crystallization of the salt from aqueous solution, a product was obtained which gives $[\alpha]_D^{20} = -28.5$. An analysis of this material shows that it is a hydrate with 3.0 moles of water of crystallization.

The hydrated form of brucine *l*-erythronate separates from a concentrated aqueous solution in the form of slender rectangular plates which lose water on heating. The loss in weight when the crystals were heated at 100° C in vacuum was 9.23 percent, whereas the water content of the compound $C_4H_8O_5 \cdot C_{23}H_{26}O_4N_2 \cdot 3H_2O$ is 9.25 percent. The hydrate, when heated slowly, has the same melting point as the anhydrous salt, but when heated rapidly, it melts at a much lower temperature.

Although the existence of the hydrate may account in part for the variation in the values for the optical rotation of brucine *l*-erythronate reported in the literature, some of the variation may have come from failure to take into consideration the concentration of the salt. In 1901, Ruff [6] reported specific rotations of −28.4 and −30.7 at weight concentrations of 4 and 9 percent, but he did not comment on

[4] In the event that an excess of brucine is present, several recrystallizations are required to obtain the pure salt. Apparently the excess brucine crystallizes with the aldonic acid, perhaps as a basic salt. The excess brucine, if present, can be removed by extraction of an aqueous solution of the salt with chloroform.

the exceptionally large concentration effect. Measurements in the present investigation gave specific rotations of −30.0, −31.4, and −34.6 at concentrations of 2, 4, and 10 g per 100 ml. From these values the equation $[\alpha]_D^{20} = -28.4 - 0.85C + 0.025C^2$, in which $C$ is the concentration of the anhydrous salt in water solution, may be calculated to represent the optical rotation of brucine *l*-erythronate. The measurements reported here were made with a polarimeter using a sodium light. It is noteworthy that concentrated solutions of brucine aldonates cannot be read satisfactorily with quartz-wedge saccharimeters with the ordinary light source, because the rotatory dispersion of the solution is not satisfactorily compensated by the dispersion of the quartz wedges, and the resulting color effects prevent accurate matching of the saccharimeter field.

## IV. PREPARATION OF BRUCINE-*d*-THREONATE FROM *d*-XYLOSE

The alcoholic solution of nonvolatile acids obtained from the oxidation of 7.5 g (0.05 mole) of *d*-xylose was mixed with 23 g (0.05 mole) of brucine dissolved in 100 ml of hot 95 percent alcohol. Crystallization began almost immediately; after 24 hours the crystals were collected on a filter, washed with alcohol, and dried. They weighed 20 g and had a melting point of 207°C and $[\alpha]_D^{20} = -43.7$. By evaporation of the mother liquor, a second crop of crystals weighing 3.2 g was obtained. The second mother liquor on evaporation gave a crystalline residue which melted below 100° C, but failed to give any fractions which appeared to contain brucine *d*-threonate. Inasmuch as both crops of crystals reacted alkaline to litmus, the presence of an excess of brucine was suspected, possibly in the form of a basic salt. To remove the excess brucine, the two crops were combined and dissolved in 100 ml of water, and the aqueous solution was extracted with a total of 150 ml of chloroform in four portions. The chloroform extract was discarded, whereas the water solution was evaporated under reduced pressure to a semifluid crystalline residue which was mixed with 15 ml of isopropyl alcohol. After several hours the resulting crystals were collected on a filter, washed with ethyl alcohol, and dried. The crude product, brucine *d*-threonate, weighed 8.5 g, melted at 210° C, and gave $[\alpha]_D^{20} = -29.4$. In addition to this, 5.3 g of crude brucine *d*-threonate was obtained by concentration of the mother liquors followed by the addition of absolute alcohol.

The yield, approximately 45 percent, is somewhat higher than that obtained by Nef, Hedenberg, and Glattfeld [5] from the oxidation of *d*-xylose with air.

After recrystallization from 30 parts of boiling 95 percent ethyl alcohol and air-drying, anhydrous brucine *d*-threonate was obtained. The anhydrous material melts at 214° to 216° C.

The specific rotation of brucine *d*-threonate[6] was found to vary widely with concentration; specific rotations of −30.2, −31.7, and −35.0 were obtained for aqueous solutions containing 2, 4, and 10 g, respectively, per 100 ml. The equation $[\alpha]_D^{20} = -28.5 - 0.9\ C + 0.025\ C^2$ (in which $C$ is the grams of anhydrous salt per 100 ml of water solution) was calculated from these values. This equation is nearly the

[6] J. U. W. Nef, Liebigs Ann. Chem. **403**, 259, 266 (1914) reported $[\alpha]_D^{25} = -32.4$ ($H_2O$, $C=4$).

same as that representing the optical rotation of brucine *l*-erythronate. Hence brucine *l*-erythronate and brucine *d*-threonate cannot be distinguished by means of optical rotation measurements. Brucine *d*-threonate on recrystallization from water gave a monohydrate rather than a trihydrate as in the case of brucine *l*-erythronate. Brucine *d*-threonate monohydrate crystallizes in flat rectangular prisms which differ in appearance from the needlelike prismatic crystals of brucine *l*-erythronate trihydrate. The sample of brucine *d*-threonate monohydrate gave the following analysis: Calculated for $C_4H_8O_5 \cdot C_{23}H_{26}O_4N_2 \cdot H_2O$: C, 59.11; H, 6.61; $H_2O$, 3.28. Found: C. 59.00; H, 6.57; $H_2O$ (loss at 100° C), 3.16.

## V. CONVERSION OF BRUCINE *l*-ERYTHRONATE OR *d*-THREONATE TO THE CORRESPONDING ACID

The brucine salt was converted to the free acid by treating a concentrated aqueous solution of the salt with an equivalent quantity of 0.5 *N* barium hydroxide solution. The brucine set free by the barium hydroxide was extracted from the aqueous solution with chloroform. The aqueous solution containing the barium salt was heated to boiling, and standardized sulfuric acid was added in amount equivalent to the barium hydroxide originally used. The resulting barium sulfate was separated, and the aqueous filtrate was evaporated to dryness. After heating 18 hours at 100° C, the residue was distilled in high vacuum to yield the crystalline gamma lactone. If seed crystals are available, the distillation can be omitted and the lactone can be separated from the residue by extraction with ethyl acetate. The ethyl acetate solution on the addition of ether yielded the crystalline lactone after seeding.

## VI. PREPARATION OF CADMIUM *l*-XYLONATE-CADMIUM BROMIDE FROM *l*-SORBOSE

The alcoholic solution of nonvolatile acids obtained from the oxidation of 9 g (0.05 mole) of *l*-sorbose was evaporated under reduced pressure to a thin sirup, which was diluted with 50 ml of water. The aqueous solution was heated to boiling and digested for 30 minutes with 4.3 g (0.025 mole), of cadmium carbonate and, after the addition of 8.6 g of cadmium bromide tetrahydrate, the resulting solution was filtered. Ethyl alcohol was added to the filtrate until two liquid phases began to appear, whereupon the solution was seeded with cadmium *l*-xylonate-cadmium bromide [8] and was placed in the refrigerator. After 1 day the resulting crystals were separated, washed with aqueous alcohol, and dried in air. The crude cadmium *l*-xylonate-cadmium bromide thus obtained weighed 8 g. Attempts to obtain additional products from the mother liquor were unsuccessful, and the yield of cadmium *l*-xylonate-cadmium bromide, $Cd(C_5H_9O_6)_2 \cdot CdBr_2 \cdot 2H_2O$, was found to be 42.6 percent of the theoretical.

## VII. PREPARATION OF *d*-LYXONO-γ-LACTONE FROM *d*-GALACTOSE

The alcoholic solution obtained from the oxidation of 9 g (0.05 mole) of *d*-galactose was evaporated under reduced pressure to a thick sirup,

which was heated for 18 hours at 100° C. The resulting lactone was dissolved in three 50-ml portions of hot isopropyl alcohol. The alcoholic solution was concentrated to a sirup which was seeded with crystals of *d*-lyxono-γ-lactone. After 2 days, crystallization was substantially complete and the crystals were separated, washed with ethyl acetate, and dried. On evaporation the mother liquor gave additional crystals which were combined with the first crop and were recrystallized from acetone. The resulting product weighed 2.1 g, melted at 114° C, and gave $[\alpha]_D^{20}=+82.7$. These constants are in agreement with those reported by Nef, Hedenberg, and Glattfeld for *d*-lyxono-γ-lactone. The yield, 28 percent, does not differ widely from that obtained by Nef by means of oxidation of *d*-galactose with air.[6]

## VIII. PREPARATION OF CALCIUM *d*-ARABONATE FROM *d*-GLUCOSE

The alcoholic solution of nonvolatile acids obtained from the oxidation of 9 g (0.05 mole) of *d*-glucose was evaporated under reduced pressure to a thin sirup, which was diluted with 100 ml of water. The aqueous solution was heated and digested for 30 minutes with 2.5 g of calcium carbonate, and the resulting solution was filtered. Ethyl alcohol was added to the filtrate until two liquid phases began to appear, whereupon the solution was seeded with calcium *d*-arabonate and allowed to stand in the refrigerator. After 1 day the crystals were separated, washed with aqueous alcohol, and dried in air. The crude *d*-arabonate weighed 8 g. After recrystallization from hot water by the addition of alcohol, 7.7 g of pure calcium *d*-arabonate $Ca(C_5H_9O_6)_2 \cdot 5H_2O$ was obtained. This is 67 percent of the yield theoretically possible. The identity of the product was established by conversion to *d*-arabono-γ-lactone.

## IX. REFERENCES

[1] J. U. W. Nef, Liebigs Ann. Chem. **403,** 204 (1914).
[2] O. Spengler and A. Pfannenstiel, Z. Ver. deut. Zucker-Ind. **85,** 546 (1933).
[3] C. Neuberg and H. Collatz, Cellulosechem. **17,** 125 (1936).
[4] N. K. Richtmyer, R. M. Hann, and C. S. Hudson, J. Am. Chem. Soc. **61,** 340, 343 (1939).
[5] J. U. W. Nef, O. F. Hedenberg, and J. W. E. Glattfeld, J. Am. Chem. Soc. **39,** 1638 (1917).
[6] O. Ruff, Ber deut. chem. Ges. **34,** 1368 (1901).
[7] C. Neuberg and E. Hirschberg, Biochem. Z. **27,** 333 (1910).
[8] E. Fischer and O. Ruff, Ber. deut. chem. Ges. **33,** 2145 (1900).

WASHINGTON, July 1, 1942.

[6] J. U. W. Nef, Liebigs Ann. Chem. **403,** 247 (1914), reported 27.4 g of lactone sirup from 100 g of *d*-galactose, which, on further treatment, gave 18.4 g of crystalline *d*-lyxono-γ-lactone. The latter corresponds to a 22-percent yield.

U. S. DEPARTMENT OF COMMERCE NATIONAL BUREAU OF STANDARDS

RESEARCH PAPER RP1498

*Part of Journal of Research of the National Bureau of Standards, Volume 29, September 1942*

# CHARACTERISTICS OF WIDE-ANGLE AIRPLANE-CAMERA LENSES

By Francis E. Washer

ABSTRACT

The relative illumination in the focal plane was measured for a number of wide-angle airplane-camera lenses, using a method depending upon the determination of the light-transmitting area of the lens effective at definite orientations of the lens. A new factor dependent on the lens design was found to be operative in reducing the values of the relative illumination in the unvignetted portion of the field for certain types of lenses. Determinations of the resolving power were also made and showed considerable variation in performance with type of lens. The effect of basing the distortion values upon the calibrated focal length instead of the equivalent focal length was determined.

CONTENTS

| | Page |
|---|---|
| I. Introduction | 233 |
| II. Relative illumination in the focal plane | 234 |
| III. Resolving power | 239 |
| IV. Distortion | 242 |

## I. INTRODUCTION

In the production of aerial photographs for use in mapping, the negative size established in the United States Department of Agriculture is 9 by 9 inches, and a lens of 8¼-inch focal length is recommended.[1] This combination produces negatives that are suitable for both planimetric and topographic mapping. However, some Government mapping agencies, such as the United States Geological Survey, are interested in producing more accurate topographic maps than can be obtained with this combination, and they have encouraged the development of short-focal-length lenses capable of producing usable imagery over a greater angular field for the same, or smaller, negative size than obtains for the typical 8¼-inch lens. Negatives produced by these wide-angle lenses are especially useful in topographic mapping, because the stereoscopic relief for contour work increases as the angle separating the image from the center of the negative increases. In the past 2 years numerous short-focal-length lenses, whose half-angular field ranged from 40° to 50°, have been submitted to this Bureau for examination to determine their suitability. An unusual opportunity was accordingly offered for studying the characteristics of a great variety of wide-angle lenses, and the results are presented in this paper.

[1] United States Department of Agriculture Specification A-APC-1102 (as approved March 1940).

## II. RELATIVE ILLUMINATION IN THE FOCAL PLANE

The present trend toward the use of wide-angle lenses in airplane photography has renewed interest in one aspect of lens performance that previously did not demand serious attention, namely, illumination in the focal plane. The latitude in film sensitivity is such that, when the half angle of the area imaged by the lens does not exceed 30°, the difference in negative density between 0° and 30° is not sufficiently great to occasion concern. However, if the half angle of the lens increases to 45°, the difference in illumination between the center and extreme portion of the negative becomes serious, since the center of the negative is overexposed, whereas the extremes are underexposed.

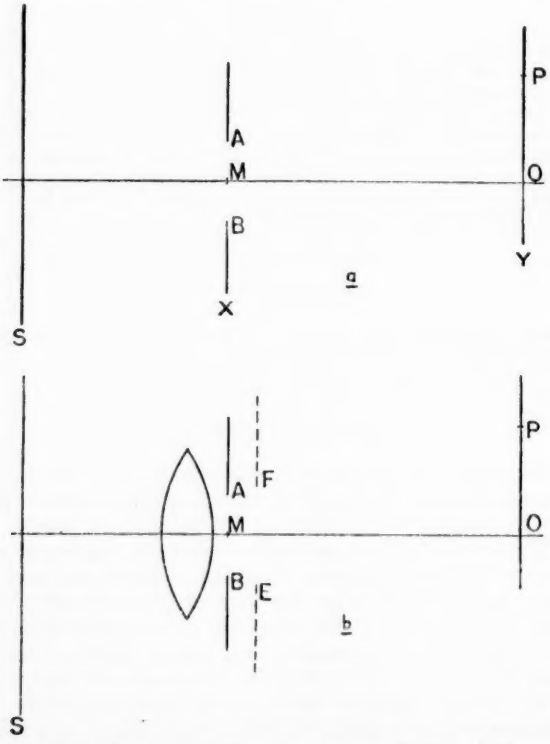


FIGURE 1.—*Schematic drawing to illustrate change of illumination with angle* $\theta$.
(a) *AB*, opening in plane *X*; (b) *AB*, opening in plane *X*; *EF*, entrance pupil of lens, *L*.

Several factors are operative in producing a reduction in the amount of light received by a given unit area in the focal plane. The first of these is illustrated in figure 1, *a*. Let light from a distant uniform extended source, *S*, pass through the circular opening, *AB*, in the opaque plane, *X*. Let *M* be the midpoint of the opening, and *O* the intersection of the normal *MO* drawn to the plane *Y* that is parallel to plane *X*. Let *P* be any point in plane *Y*, such that a line joining *M* and *P* makes angle $\theta$ with *OM*; then it can be shown to a

satisfactory degree of approximation that the relationship between the illumination $E_p$ at point $P$ and $E_0$ at point $O$ is

$$E_p = E_0 \cos^4 \theta. \tag{1}$$

It has been customary to extend the coverage of this relationship to the case where the entrance pupil, $EF$, of the lens serves as the circular opening, figure 1, *b*. This is a reasonable assumption, because the entrance pupil of the lens is simply the image of the diaphragm stop opening as formed by that part of the optical system lying between the diaphragm and the object, and as such should behave as the simple circular opening illustrated in figure 1, *a*. It is shown later in this paper that this is not always true. The second major factor is the encroachment of the lens boundary into the light path. This reduction of the effective diaphragm area by the lens mounting is called vignetting. Until the development of wide-angle lenses, vignetting was the principal factor in reducing the illumination at the edge of the picture. The illumination at 30° is 56 percent of the axial illumination (from eq. 1), and this reduction is not sufficient to impair seriously the quality of the negative if no vignetting is present. However, when the half angle is increased to 45°, the illumination at 45° is 25 percent of that on the axis when no vignetting is present. Hence the vignetting must be kept small indeed if good negatives are to be made with wide-angle lenses. It is difficult to make good use of negatives made when the ratio of illumination in different parts of the focal plane exceeds 8 to 1. It was therefore considered worthwhile to determine by measurement the relative illumination in the focal plane for a number of wide-angle mapping lenses. During the course of this investigation, an additional factor affecting the illumination in the focal plane was discovered and found to be associated with the design of the lens.

An indirect method is used in determining the relative illumination in different parts of the focal plane. Referring to figure 1, *a*, it is evident that the expression for relative illumination may be written:

$$E_p = (A_\theta / A_0) E_0 \cos^3 \theta, \tag{2}$$

where $A_0$ is the area of the opening $AB$ in the plane $X$, and $A_\theta$ is the projected area of $AB$ as viewed at the angular obliquity $\theta$. For figure 1, *a*, $A_\theta = A_0 \cos \theta$, but for a lens whose effective light-transmitting area is reduced by vignetting or other causes $A_\theta < A_0 \cos \theta$. A method was therefore devised to measure $A_\theta$ and $A_0$.

The lens was mounted on a stand that permitted rotation about a vertical axis. The lens diaphragm was set at the selected stop opening, and the edges of this opening were illuminated from the rear of the lens by a fixed source. Photographs of the stop opening were made with an auxiliary camera in front of the lens. The lens under test and the camera lens were made as nearly coaxial as possible for the zero setting of the lens. The position of the lens was adjusted with respect to the vertical axis of rotation until no transverse displacement of the diaphragm image was noticeable when the lens under test was rotated from the zero position to the limit of its range. Photographs of the diaphragm opening were taken at 5° intervals from the centered position to 45° from the axis. Prints were made from these negatives, and the area of each image was measured with

a planimeter. The ratio of the area, $A_\theta$, at any angle, $\theta$, to the area, $A_0$ of the axial image is taken as equivalent to the ratio of the effective aperture area at the given angle to the axial aperture area. This ratio, $A_\theta/A_0$, is therefore the same as that appearing in the expression for relative illumination in the focal plane, as written in equation 2. The values obtained are shown in table 1 and given graphically in figure 2.

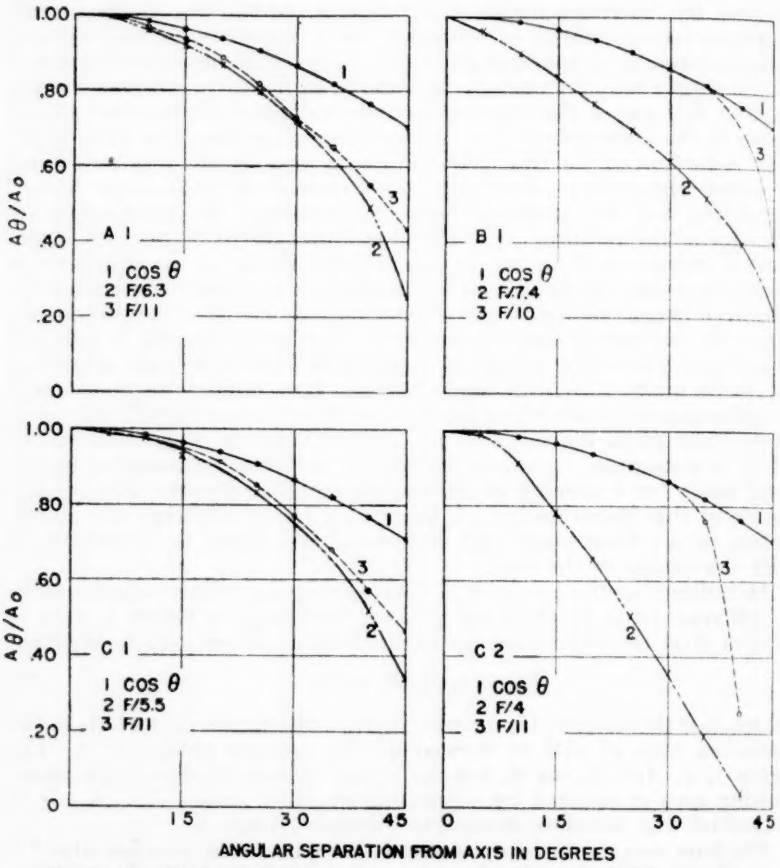


FIGURE 2.—*Ratio of effective aperture area, $A_\theta$, to axial aperture area, $A_0$.*

TABLE 1.—*Ratio of $A_\theta$ to $A_0$ for four lenses*[1]

| Manufacturer and lens type number | Relative aperture | Angular separation from axis | | | | | | | | | |
|---|---|---|---|---|---|---|---|---|---|---|---|
| | | 0° | 5° | 10° | 15° | 20° | 25° | 30° | 35° | 40° | 45° |
| *A1* | 6.3 | 1.000 | 0.995 | 0.962 | 0.923 | 0.867 | 0.799 | 0.725 | 0.637 | 0.487 | 0.247 |
| | 11 | 1.000 | ------ | .969 | .944 | .886 | .820 | .731 | .647 | .550 | .431 |
| *B1* | 7.4 | 1.000 | .959 | .906 | .844 | .775 | .698 | .617 | .520 | .402 | .218 |
| | 10 | 1.000 | .982 | .974 | .959 | .928 | .903 | .880 | .819 | .704 | .390 |
| *C1* | 5.5 | 1.000 | .988 | .878 | .934 | .900 | .835 | .741 | .660 | .520 | .343 |
| | 11 | 1.000 | ------ | ------ | ------ | .916 | .852 | .772 | .675 | .574 | .464 |
| *C2* | 4 | 1.000 | .993 | .913 | .783 | .659 | .507 | .352 | .192 | .037 | ... |
| | 11 | 1.000 | ------ | .974 | .957 | .927 | .893 | .876 | .748 | .244 | ... |

$A_0$=area of lens diaphragm opening; $A_\theta$=area of effective diaphragm opening at angle $\theta$ from lens axis.

Vignetting by the lens boundary becomes effective at a small angle for lenses *B1* and *C2* when used at the maximum $f$/value, and consequently the curve of $A_\theta/A_0$ departs from cos $\theta$ at the start, as may be seen in the number 2 curves in figure 2. However, when *B1* is stopped down to $f/10$, the cosine law is followed out to 35°, at which point vignetting begins and curve 3 falls away from curve 1. For *C2* at $f/11$, the cosine law is followed to 30°, and vignetting becomes effective at that point, as evidenced by curve 3, branching down from curve 1.

Since the relation $A_\theta/A_0 = \cos\theta$ was found to be followed in the unvignetted region for lenses *B1* and *C2*, it is somewhat disconcerting to find that for lenses *A1* and *C1* the values of $A_\theta/A_0$ are consistently below the corresponding values of cosine $\theta$. This departure is present at both aperture ratios, although it is somewhat less pronounced at the smaller aperture ratio. For lens *A1*, vignetting begins at 35° for aperture $f/6.3$ and at 40° for aperture $f/11$. For *C1*, vignetting begins at 40° for aperture $f/5.5$, and at 45° for aperture $f/11$. Hence this departure of $A_\theta/A_0$ from the corresponding value of cosine $\theta$ is present in the unvignetted region, and the amount of this departure is greater than can reasonably be assigned to experimental error. This is shown for a lens of the *A1* type in table 2, where the percentage departure of values of $A_\theta/A_0$ from corresponding values of cosine $\theta$ increases progressively with increasing angle. Since the errors in measurement do not on the average exceed $\pm 1.5$ percent, this departure of $A_\theta/A_0$ from cosine $\theta$ is markedly greater than can be attributed to error. For example, the departure at 30° is $-16.3$ percent at aperture $f/6.3$. This is definitely in the unvignetted region and must arise from some cause that has not heretofore been generally recognized. This condition did not prevail for all lenses studied. It therefore seemed probable that such variation in behavior could only arise from differences in the lens design. To verify this hypothesis, a series of computations was made for a lens of the *A1* type. These computations consisted in tracing rays that were parallel and of various linear separations in the object space through that portion of the lens lying between the diaphragm opening and the object space. This was done for axial rays and for rays in the plane of the optic axis that made an angle of $\theta$ with the axis. The linear separation of each ray from the axis at the point where it passed through the plane of the diaphragm was determined, and pairs of rays were selected that passed through the diaphragm at the same distance from the axis. The ratio of the separation $d_\theta$ for each pair at angle $\theta$ to the separation $d_0$ for each corresponding axial pair in the object space was obtained. It was found that this ratio, $d_\theta/d_0$, was less than the cosine $\theta$. For $\theta = 30°$, the percentage departure at $f/6$ was $-10.3$; at $f/11$, $-9.5$; and at $f/20$, $-9.2$. These values indicate that the effect is a maximum at large aperture but decreases slightly with diminishing aperture. Similar behavior is seen in table 2 for $A_{30°}/A_0$, where it is apparent that the percentage departure from the cosine value is greater at $f/6.3$ than at $f/11$.

The departure from the cosine value is greater for $A_{30°}/A_0$ than for $d_{30°}/d_0$. This discrepancy is undoubtedly due to the differences in the objects projected. In the first instance we are dealing with a circular area, whereas in the second only a single diameter is considered. It is probable that the projection of additional diameters at several inclinations to the initial diameter would permit an evaluation of the

areal effect. However, the present computations for a single diameter clearly indicate that the ratio $A_\theta/A_0$ is affected by the lens design.

TABLE 2.—*Deviation of $A_\theta/Af$ from cosine $\theta$ for lens A1*

| Relative aperture | Quantity | Angular separation from the axis | | | | | | | | |
|---|---|---|---|---|---|---|---|---|---|---|
| | | 0° | 10° | 15° | 20° | 25° | 30° | 35° | 40° | 45° |
| 6.3 | Cosine $\theta$ | 1.000 | +0.985 | +0.966 | +0.940 | +0.906 | +0.866 | +0.819 | +0.766 | +0.707 |
| | $A_\theta/A_0$ | 1.000 | +.962 | +.923 | +.867 | +.799 | +.725 | +.637 | +.487 | +.247 |
| | Cos $\theta - A_\theta/A_0$ | 0.000 | +.023 | +.043 | +.073 | +.107 | +.141 | +.182 | +.279 | +.460 |
| | Percentage of deviation | .0 | −2.3 | −4.4 | −7.8 | −11.8 | −16.3 | −22.2 | −36.4 | −65.1 |
| | $A_\theta/A_0$ | 1.000 | +.969 | +.944 | +.886 | +.820 | +.731 | +.647 | +.550 | +.431 |
| | Cos $\theta - A_\theta/A_0$ | 0.000 | +.016 | +.022 | +.054 | +.086 | +.135 | +.172 | +.216 | +.276 |
| | Percentage of deviation | .0 | −1.6 | −2.3 | −5.7 | −9.5 | −15.6 | −21.0 | −28.2 | −39.0 |

Finally, the relative illumination in the focal plane is obtained by multiplying the values of $A_\theta/A_0$ shown in table 1 by $\cos^3\theta$. These values are given in table 3, and a graphic illustration for each lens is given in figure 3. Curve 1 in each box shows the value of $\cos^4\theta$ and is

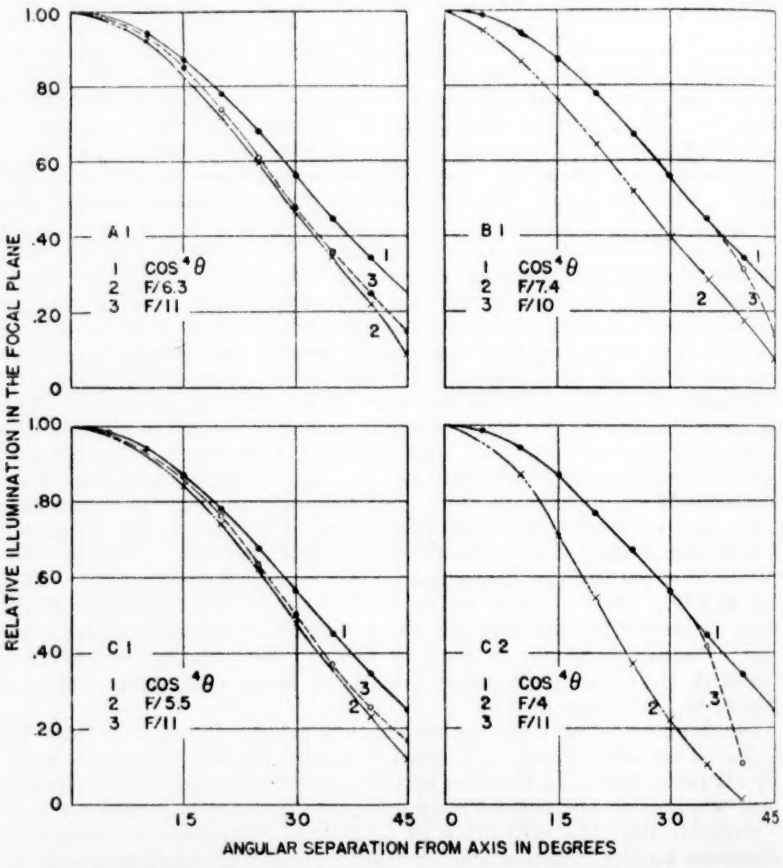


FIGURE 3.—*Relative illumination in the focal plane, reflection losses ignored.*

inserted for ready reference. The relation $E_p = E_0 \cos^4\theta$ is followed within the limits of experimental errors by lenses *B1* and *C2* until vignetting begins, whereas $E_p < E_0 \cos^4\theta$ for lenses *A1* and *C1* throughout the entire range. It is accordingly clear that the loss in illumination inherent in the lens design is greater for *A1* and *C1* than the loss resulting from vignetting.

TABLE 3.—*Relative illumination in the focal plane*

| Manufacturer and lens type number | Relative aperture | Angular separation from the axis | | | | | | | | | |
|---|---|---|---|---|---|---|---|---|---|---|---|
| | | 0° | 5° | 10° | 15° | 20° | 25° | 30° | 35° | 40° | 45° |
| *A1* | f 6.3 | 1.000 | 0.984 | 0.919 | 0.832 | 0.719 | 0.595 | 0.471 | 0.350 | 0.219 | 0.087 |
| | 11 | 1.000 | ..... | .926 | .851 | .735 | .610 | .475 | .356 | .247 | .152 |
| *B1* | f 7.4 | 1.000 | .948 | .865 | .761 | .643 | .520 | .401 | .286 | .181 | .077 |
| | 10 | 1.000 | .971 | .930 | .864 | .770 | .672 | .572 | .450 | .316 | .138 |
| *C1* | f 5.5 | 1.000 | .977 | .934 | .842 | .747 | .622 | .481 | .363 | .234 | .121 |
| | 11 | 1.000 | ..... | ..... | ..... | .760 | .634 | .501 | .371 | .258 | .164 |
| *C2* | f 4 | 1.000 | .982 | .872 | .706 | .547 | .377 | .229 | .106 | .017 | ..... |
| | 11 | 1.000 | ..... | .930 | .802 | .769 | .665 | .569 | .411 | .110 | ..... |

The values of the relative illumination obtained by this method of measurement do not take into account possible loss in light resulting from absorption in the glass or from reflections at the surfaces. However, the values present a clear picture of the best possible performance of a given lens.

## III. RESOLVING POWER

In the study of resolving power and distortion, the precision lens-testing camera described by Gardner[2] and Case was used. The method of selecting the image plane of best average definition was the same as that described in a previous paper.[3] The principal modification in the equipment was the addition of three collimators that extended the image region studied from 30° to 45° from the axis.

The results of the measurements on resolving power are shown in table 4. In all cases, except for lenses 15, 17, 19, 22, 23, and 24, the *f*/values, listed in column 4, are the maximum. For lenses of a given type and focal length, the highest value of the axial resolving power is nearly constant. The variations on the axis that appear in table 4 resulted from the necessity of selecting an image plane that yielded usable imagery throughout the entire field. Under these conditions, the resolving power on the axis sometimes falls below the maximum of which it is capable.

[2] J. Research NBS **18**, 449 (1937) RP984.
[3] J. Research NBS **22**, 729 (1939) RP1216.

TABLE 4.—*Resolving power in the plane of best average definition for 26 wide-angle airplane-camera lenses*

| Manufacturer and lens type number | Lens number | Equivalent focal length | Relative aperture or f/value | Tangential resolving power in lines per millimeter (angular distance from axis) | | | | | | | | | | Radial resolving power in lines per millimeter (angular distance from axis) | | | | | | | | | |
|---|---|---|---|---|---|---|---|---|---|---|---|---|---|---|---|---|---|---|---|---|---|---|---|
| | | | | 0° | 5° | 10° | 15° | 20° | 25° | 30° | 35° | 40° | 45° | 0° | 5° | 10° | 15° | 20° | 25° | 30° | 35° | 40° | 45° |
| 1 | 2 | 3 | 4 | 5 | 6 | 7 | 8 | 9 | 10 | 11 | 12 | 13 | 14 | 15 | 16 | 17 | 18 | 19 | 20 | 21 | 22 | 23 | 24 |
| *A1* | 1 | 132.49 | 6.3 | 63 | 63 | 63 | 63 | 32 | 22 | 16 | 16 | 8 | 8 | 63 | 63 | 63 | 63 | 63 | 44 | 44 | 44 | 44 | 22 |
| | 2 | 132.55 | 6.3 | 24 | 32 | 32 | 32 | 32 | 24 | 16 | 16 | 16 | 12 | 24 | 32 | 48 | 32 | 32 | 32 | 32 | 32 | 32 | 24 |
| | 3 | 132.33 | 6.3 | 56 | 56 | 56 | 40 | 40 | 28 | 20 | 7 | 7 | 10 | 56 | 56 | 56 | 56 | 56 | 56 | 40 | 28 | 20 | 14 |
| | 4 | 132.21 | 6.3 | 63 | 63 | 44 | 44 | 44 | 32 | 32 | 32 | 22 | 11 | 63 | 63 | 44 | 44 | 44 | 32 | 32 | 32 | 22 | 32 |
| | 5 | 132.63 | 6.3 | 32 | 32 | 22 | 22 | 32 | 22 | 22 | 32 | 32 | 16 | 22 | 22 | 16 | 16 | 16 | 16 | 22 | 44 | 44 | 32 |
| | 6 | 131.05 | 6.3 | 44 | 44 | 44 | 44 | 44 | 44 | 32 | 16 | 8 | 11 | 63 | 44 | 44 | 63 | 44 | 44 | 32 | 22 | 16 | 16 |
| | 7 | 132.11 | 6.3 | 64 | 64 | 44 | 32 | 16 | 16 | 16 | 11 | 11 | 11 | 64 | 64 | 44 | 44 | 44 | 32 | 32 | 32 | 32 | 22 |
| | 8 | 131.77 | 6.3 | 44 | 44 | 44 | 44 | 32 | 32 | 32 | 32 | 22 | 16 | 44 | 44 | 44 | 44 | 44 | 44 | 32 | 32 | 32 | 22 |
| | 9 | 101.29 | 6.3 | 58 | 58 | 58 | 58 | 58 | 58 | 41 | 29 | 21 | 14 | 58 | 41 | 41 | 41 | 58 | 58 | 41 | 29 | 21 | 14 |
| | 10 | 152.27 | 6.3 | 56 | 56 | 40 | 28 | 20 | 20 | 29 | 20 | 20 | 14 | 56 | 56 | 40 | 40 | 40 | 28 | 28 | 28 | 20 | 14 |
| *A2* | 11 | 166.23 | 11 | 40 | 40 | 40 | 40 | 28 | 20 | 10 | 7 | 14 | ..... | 40 | 40 | 56 | 40 | 20 | 20 | 40 | 28 | ..... | ..... |
| | 12 | 166.11 | 11 | 50 | 50 | 71 | 50 | 35 | 25 | 18 | 13 | 13 | ..... | 50 | 50 | 71 | 35 | 25 | 25 | 50 | 18 | ..... | ..... |
| *B1* | 13 | 129.23 | 10 | 23 | 32 | 45 | 45 | 45 | 45 | 32 | 32 | 32 | 11 | 23 | 32 | 65 | 23 | 11 | 8 | 8 | 11 | 32 | 11 |
| *B2* | 14 | 145.42 | 10 | 40 | 80 | 40 | 20 | 10 | 14 | 20 | 20 | 14 | 7 | 40 | 58 | 58 | 20 | 14 | 14 | 40 | 29 | ..... | ..... |
| *B3* | 15 | 109.01 | 11 | 56 | 56 | 40 | 28 | 20 | 20 | 20 | 20 | 14 | 3.5 | 56 | 56 | 40 | 28 | 14 | 7 | 5 | 20 | 30 | 3.5 |
| | 16 | 151.44 | 8 | 28 | 28 | 55 | 19 | 19 | 14 | 14 | 7 | ..... | ..... | 28 | 39 | 55 | 14 | 7 | 7 | 7 | 7 | 14 | ..... |
| | 17 | 149.23 | 16 | 20 | 39 | 56 | 56 | 28 | 20 | 28 | 28 | 20 | ..... | 20 | 39 | 56 | 28 | 10 | 7 | 7 | 20 | 14 | ..... |
| | 18 | 163.39 | 8 | 36 | 36 | 51 | 18 | 13 | 13 | 13 | 18 | ..... | ..... | 36 | 36 | 56 | 18 | 9 | 7 | 7 | 18 | 7 | ..... |
| | 19 | 165.10 | 11 | 56 | 56 | 28 | 20 | 14 | 10 | 10 | 10 | 3.5 | ..... | 56 | 56 | 28 | 14 | 5 | 5 | 5 | 5 | 20 | ..... |
| *C1* | 20 | 115.99 | 5.5 | 51 | 72 | 51 | 25 | 25 | 25 | 36 | 25 | 13 | 13 | 51 | 72 | 51 | 51 | 36 | 25 | 36 | 36 | 36 | 36 |
| *C2* | 21 | 153.90 | 4 | 54 | 76 | 54 | 27 | 19 | 19 | 14 | 14 | 10 | ..... | 54 | 76 | 27 | 10 | 10 | 7 | 19 | 14 | ..... | ..... |
| *D1* | 22 | 158.28 | 22 | 18 | 36 | 54 | 54 | 54 | 24 | 14 | 10 | 20 | 2 | 36 | 54 | 54 | 54 | 18 | 14 | 6 | 8 | 6 | 8 |
| | 23 | 158.07 | 22 | 18 | 36 | 36 | 54 | 42 | 28 | 28 | 28 | 18 | 6 | 14 | 18 | 36 | 54 | 42 | 14 | 14 | 14 | 48 | 6 |
| | 24 | 158.28 | 22 | 36 | 36 | 54 | 54 | 36 | 36 | 28 | 28 | 24 | 4 | 18 | 36 | 54 | 54 | 36 | 12 | 8 | 12 | 42 | 6 |
| *E1* | 25 | 98.92 | 6.3 | 85 | 85 | 59 | 42 | 42 | 30 | 30 | 30 | 21 | 15 | 85 | 85 | 85 | 59 | 59 | 59 | 59 | 42 | 42 | 21 |
| *F1* | 26 | 87.22 | 22 | 48 | 48 | 48 | 48 | 34 | 34 | 24 | 24 | 17 | 17 | 48 | 48 | 48 | 48 | 48 | 34 | 34 | 34 | 24 | 24 |

The curves shown in figures 4 and 5 illustrate the tangential and radial resolving powers for the lenses described in table 4. Identifications are given in the upper right-hand corner of each box. Where more than one lens of a given type has been studied under identical conditions, the curves show the averaged values for the group instead of for a single lens. The solid-line curves show the tangential and the dotted-line curves, the radial resolving power. The separation of the two curves illustrates the astigmatic difference in the given image plane at each angle.

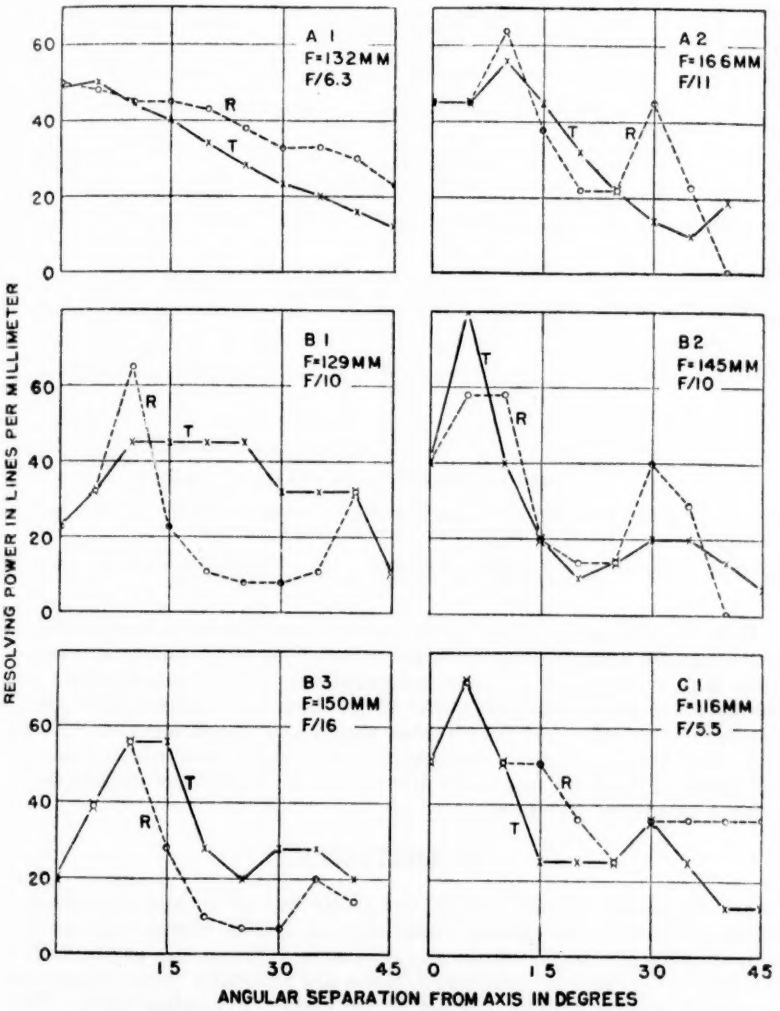


FIGURE 4.—*Resolving power in the plane of best average definition for six types of wide-angle airplane-camera lenses.*

*T*, Tangential resolving power; *R*, radial resolving power. Lens identification by manufacturer and type in upper right-hand corner of each part.

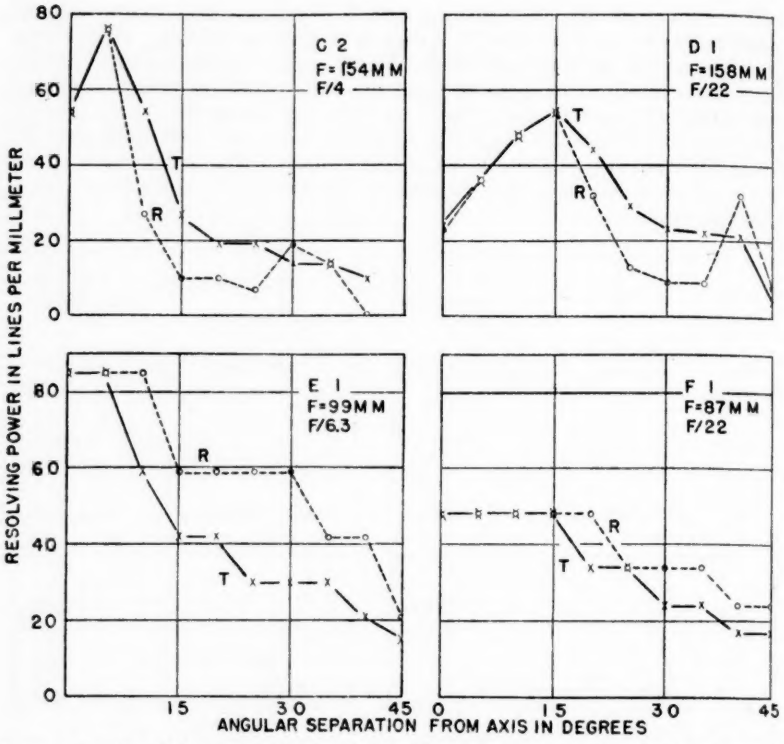


FIGURE 5.—*Resolving power in the plane of best average definition for four types of wide-angle airplane-camera lenses.*

*T*, Tangential resolving power; *R*, radial resolving power. The lens identification by the manufacturer and the type are given in upper right-hand corner of each part.

Definite standards of performance have not yet been established by Government mapping agencies for wide-angle airplane-camera lenses. This is primarily due to their comparatively recent introduction into the field of airplane mapping and to the lack of sufficient data for the determination of what constitutes reasonable requirements. Tentative specifications [4] set a minimum resolving power of 14 lines per millimeter for a focal length of 100 mm and 10 lines per millimeter for a focal length of 131 mm.

## IV. DISTORTION

For the same angular range, the distortion of wide-angle airplane-camera lenses is no greater than that of lenses whose angular field ranges from 30° to 35° from the lens axis. When the entire field of the wide-angle lens is considered, there are generally larger distortions present than are usually permitted for lenses of smaller field. However, the advantages that result from the greater field are such as to outweigh the need for low distortion. The distortions are kept as low

[4] These specifications are contained in a communication to this Bureau from the Department of the Interior, Geological Survey, in July 1940.

as possible and as more of the lenses are made, it is reasonable to suppose that means of reducing the distortion will be found. In the tentative specifications mentioned earlier (see footnote 4), the maximum allowable distortion referred to the equivalent focal length is $\pm 0.20$ mm for 100-mm lenses and $\pm 0.30$ mm for 130-mm lenses.

Table 5 lists the distortion for the lenses whose resolving powers are listed in table 4. For a given lens whose distortion is shown in table 5, the resolving power is given under the same number in table 4; column 3 gives the equivalent focal length, on the basis of which the values of the distortion shown in columns 4 to 12 are computed. Column 13 gives the calibrated focal length, on the basis of which the values of the distortion shown in columns 14 to 22 are computed.

TABLE 5.—*Distortion of 26 wide angle airplane camera lenses*

| Manufacturer and lens type number | Lens number | Equivalent focal length | Distortion referred to the equivalent focal length | | | | | | | | | Calibrated focal length | Distortion referred to the calibrated focal length | | | | | | | | |
|---|---|---|---|---|---|---|---|---|---|---|---|---|---|---|---|---|---|---|---|---|---|
| | | | 5° | 10° | 15° | 20° | 25° | 30° | 35° | 40° | 45° | | 5° | 10° | 15° | 20° | 25° | 30° | 35° | 40° | 45° |
| 1 | 2 | 3 | 4 | 5 | 6 | 7 | 8 | 9 | 10 | 11 | 12 | 13 | 14 | 15 | 16 | 17 | 18 | 19 | 20 | 21 | 22 |
| | | *mm* | *mm* | *mm* | *mm* | *mm* | *mm* | *mm* | *mm* | *mm* | *mm* | *mm* | *mm* | *mm* | *mm* | *mm* | *mm* | *mm* | *mm* | *mm* | *mm* |
| | 1 | 132.49 | 0.00 | 0.00 | +0.01 | +0.01 | +0.02 | +0.03 | +0.06 | +0.04 | −0.03 | 132.51 | 0.00 | 0.00 | +0.01 | 0.00 | +0.01 | +0.02 | +0.05 | +0.02 | −0.05 |
| | 2 | 132.55 | .00 | .00 | .00 | +.01 | +.02 | +.04 | +.07 | +.06 | −.01 | 132.59 | .00 | −.01 | −.01 | −.01 | .00 | +.02 | +.04 | +.03 | −.05 |
| | 3 | 132.33 | .00 | .00 | +.01 | +.02 | +.04 | +.06 | +.07 | +.04 | −.08 | 132.33 | .00 | .00 | +.01 | +.02 | +.04 | +.06 | +.07 | +.04 | −.08 |
| | 4 | 131.93 | .00 | .00 | .00 | +.01 | +.02 | +.04 | +.05 | +.16 | −.09 | 131.97 | .00 | −.01 | −.01 | −.01 | .00 | +.02 | +.02 | +.13 | −.13 |
| *A1* | 5 | 132.63 | .00 | .00 | .00 | +.02 | +.04 | +.07 | +.09 | +.08 | −.04 | 132.66 | .00 | .00 | −.01 | +.01 | +.03 | +.05 | +.07 | +.06 | −.07 |
| | 6 | 131.05 | .00 | .00 | +.01 | +.03 | +.05 | +.09 | +.10 | +.04 | −.12 | 131.04 | .00 | .00 | .00 | +.03 | +.05 | +.10 | +.11 | +.05 | −.11 |
| | 7 | 132.11 | .00 | .00 | .00 | +.01 | +.02 | +.04 | +.04 | −.01 | −.18 | 132.03 | +.01 | +.01 | +.02 | +.04 | +.06 | +.09 | +.10 | +.06 | −.10 |
| | 8 | 131.77 | .00 | .00 | +.01 | +.03 | +.06 | +.09 | +.13 | +.11 | −.03 | 131.83 | .00 | −.01 | −.01 | +.01 | +.03 | +.06 | +.09 | +.06 | −.09 |
| | 9 | 101.29 | .00 | .00 | +.01 | +.03 | +.05 | +.09 | +.11 | +.11 | .00 | 101.35 | .00 | −.01 | −.01 | +.01 | +.02 | +.06 | +.07 | +.06 | −.06 |
| | 10 | 152.27 | .00 | .00 | +.01 | +.01 | +.02 | +.02 | .00 | −.10 | −.40 | 152.03 | +.02 | +.04 | +.07 | +.10 | +.13 | +.16 | +.17 | +.10 | −.16 |
| *A2* | 11 | 166.33 | .00 | .00 | +.01 | .00 | −.01 | −.01 | +.07 | +.26 | ..... | 166.51 | −.02 | −.03 | −.04 | −.07 | −.09 | −.11 | −.06 | +.11 | ..... |
| | 12 | 166.11 | .00 | .00 | .00 | −.02 | −.05 | −.04 | +.05 | +.21 | ..... | 166.23 | −.01 | −.02 | −.03 | −.06 | −.11 | −.11 | −.03 | +.11 | ..... |
| *B1* | 13 | 129.23 | .00 | −.01 | −.01 | −.02 | −.02 | −.03 | −.02 | .00 | +.06 | 129.25 | .00 | −.01 | −.01 | −.03 | −.03 | −.04 | −.03 | −.02 | +.04 |
| *B2* | 14 | 145.42 | .00 | .00 | +.02 | +.02 | .00 | −.04 | −.07 | +.09 | +.41 | 145.62 | −.02 | −.04 | −.03 | −.05 | −.09 | −.16 | −.21 | −.08 | +.21 |
| | 15 | 109.01 | .00 | +.01 | +.02 | +.03 | +.04 | +.05 | +.08 | +.17 | +.38 | 109.28 | −.02 | −.04 | −.05 | −.07 | −.09 | −.11 | −.11 | −.06 | +.11 |
| *B3* | 16 | 151.44 | .00 | .00 | +.02 | +.05 | +.08 | +.10 | +.15 | +.25 | ..... | 151.68 | −.02 | −.04 | −.04 | −.04 | −.03 | −.04 | −.02 | +.05 | ..... |
| | 17 | 149.23 | .00 | .00 | +.01 | +.02 | +.03 | +.04 | +.10 | +.42 | ..... | 149.56 | −.03 | −.06 | −.08 | −.10 | −.12 | −.15 | −.13 | +.14 | ..... |
| | 18 | 163.39 | .00 | .00 | +.02 | +.05 | +.07 | +.10 | +.20 | +.35 | ..... | 163.71 | −.03 | −.06 | −.06 | −.07 | −.08 | −.08 | −.02 | +.08 | ..... |
| | 19 | 165.10 | .00 | .00 | +.02 | +.05 | +.08 | +.11 | +.16 | +.26 | ..... | 165.35 | −.02 | −.04 | −.04 | −.04 | −.04 | −.03 | −.02 | +.05 | ..... |
| *C1* | 20 | 115.99 | .00 | .00 | +.02 | +.06 | +.10 | +.17 | +.24 | +.31 | +.32 | [1] | .00 | .00 | +.01 | +.03 | +.05 | +.07 | +.07 | +.04 | −.10 |
| *C2* | 21 | 153.90 | .00 | .00 | .00 | +.01 | −.01 | .00 | +.02 | +.19 | ..... | 154.03 | −.01 | −.02 | −.03 | −.04 | −.07 | −.08 | −.07 | +.08 | ..... |
| | 22 | 158.28 | .00 | .00 | −.01 | −.01 | −.01 | +.01 | +.07 | +.20 | +.50 | 158.60 | −.03 | −.06 | −.09 | −.13 | −.16 | −.17 | −.15 | +.18 | ..... |
| *D1* | 23 | 158.07 | .00 | .00 | .00 | .00 | .00 | +.02 | +.08 | +.23 | +.60 | 158.47 | −.04 | −.07 | −.10 | −.14 | −.18 | −.21 | −.20 | −.11 | +.20 |
| | 24 | 158.28 | .00 | .00 | −.01 | −.01 | −.01 | +.01 | +.06 | +.21 | +.56 | 158.64 | −.03 | −.06 | −.11 | −.14 | −.18 | −.20 | −.19 | −.09 | +.20 |
| *E1* | 25 | 98.92 | .00 | .00 | +.02 | +.04 | +.08 | +.14 | +.21 | +.26 | +.21 | 99.17 | −.02 | −.04 | −.04 | −.05 | −.04 | +.00 | +.03 | +.05 | −.04 |
| *F1* | 26 | 87.22 | .00 | .00 | .00 | −.01 | −.01 | .00 | .00 | +.02 | +.06 | 87.25 | .00 | .00 | −.01 | −.02 | −.02 | −.02 | −.02 | .00 | +.03 |

[1] Corrected by a ⅛-in. glass plate.

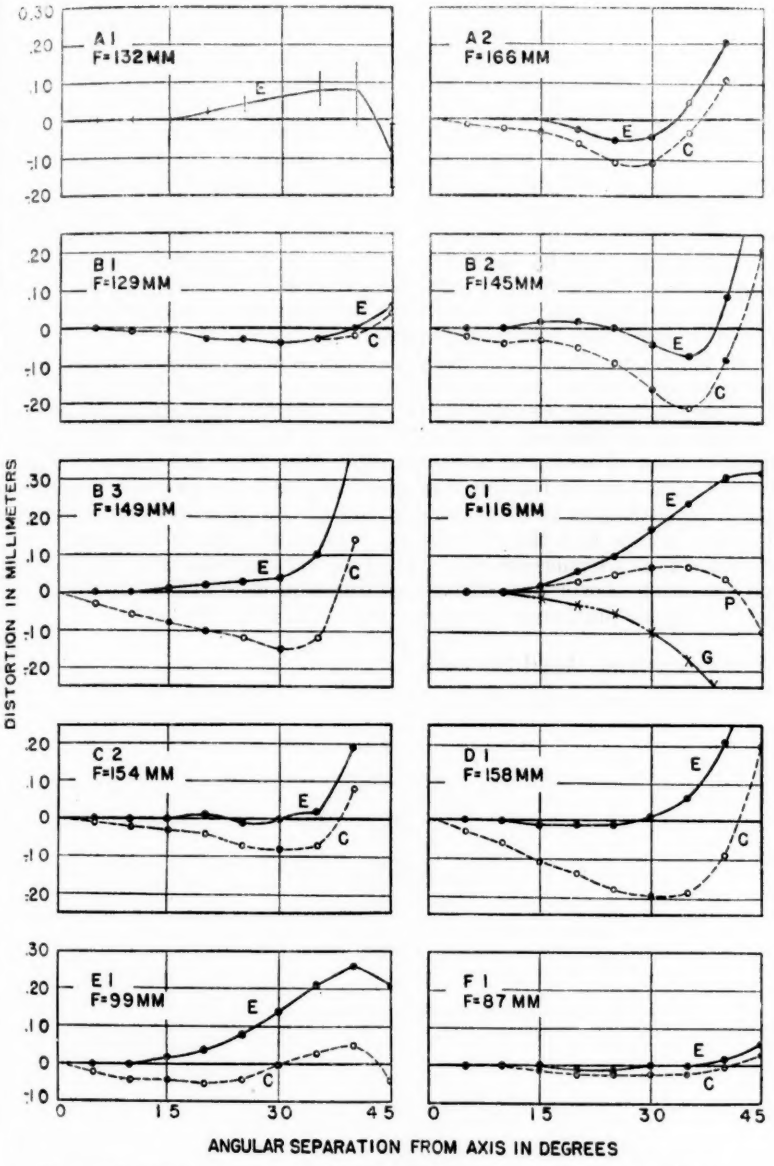


FIGURE 6.—*Distortion for 10 types of wide-angle airplane-camera lenses.*

*E*, Distortion referred to the equivalent focal length; *C*, distortion referred to the calibrated focal length. For lens *C1*; *G*, distortion for a plane-parallel plate of glass of index 1.52 and ⅛-in. thickness; *P*, distortion for combination of lens and plane-parallel glass plate. The lens identification by the manufacturer and the type are given in the upper center of each part.

474862—42——5

The value of the distortion referred to the calibrated focal length is the more significant one in evaluating the performance of a lens. The calibrated focal length is chosen to minimize the distortion and distribute it over the whole area of the image. The method of determining the calibrated focal length from the equivalent focal length and the advantages of doing so are described by Gardner.[5]

The advantage of basing distortion values on the calibrated focal length is shown in figure 6. Some idea of the range in distortion values for a given type of lens is given in box *A1*, where the average distortion of eight lenses of the same type is plotted. The range in values for each angle is given by the vertical lines. It is interesting to note that the average curve corresponds closely to the values listed for lens 3. In this instance the calibrated and equivalent focal lengths are equal and the distortion curves superpose.

For lens 20 reduction of the distortion is accomplished by the interposition of a ⅛-in. glass plate between the lens and the focal plane. In figure 6, box *C1*, the distortion curves for the lens alone, for a plane-parallel glass plate of index 1.52 and ⅛-inch thickness, and for the combination of lens and plane-parallel glass plate are given. This is, however, a lens of foreign manufacture, and the present practice in the United States is to avoid the use of the glass pressure plate between the lens and the focal plane. Lens 26, shown in figures 5 and 6, box *F1*, is a hypergon lens. It gives very satisfactory performance on resolving power and distortion, but the difficulty of manufacture and its small maximum stop opening, *f*/22, limit its use.

WASHINGTON, April 23, 1942.

[5] J. Research NBS **22**, 209 (1939) RP1177.